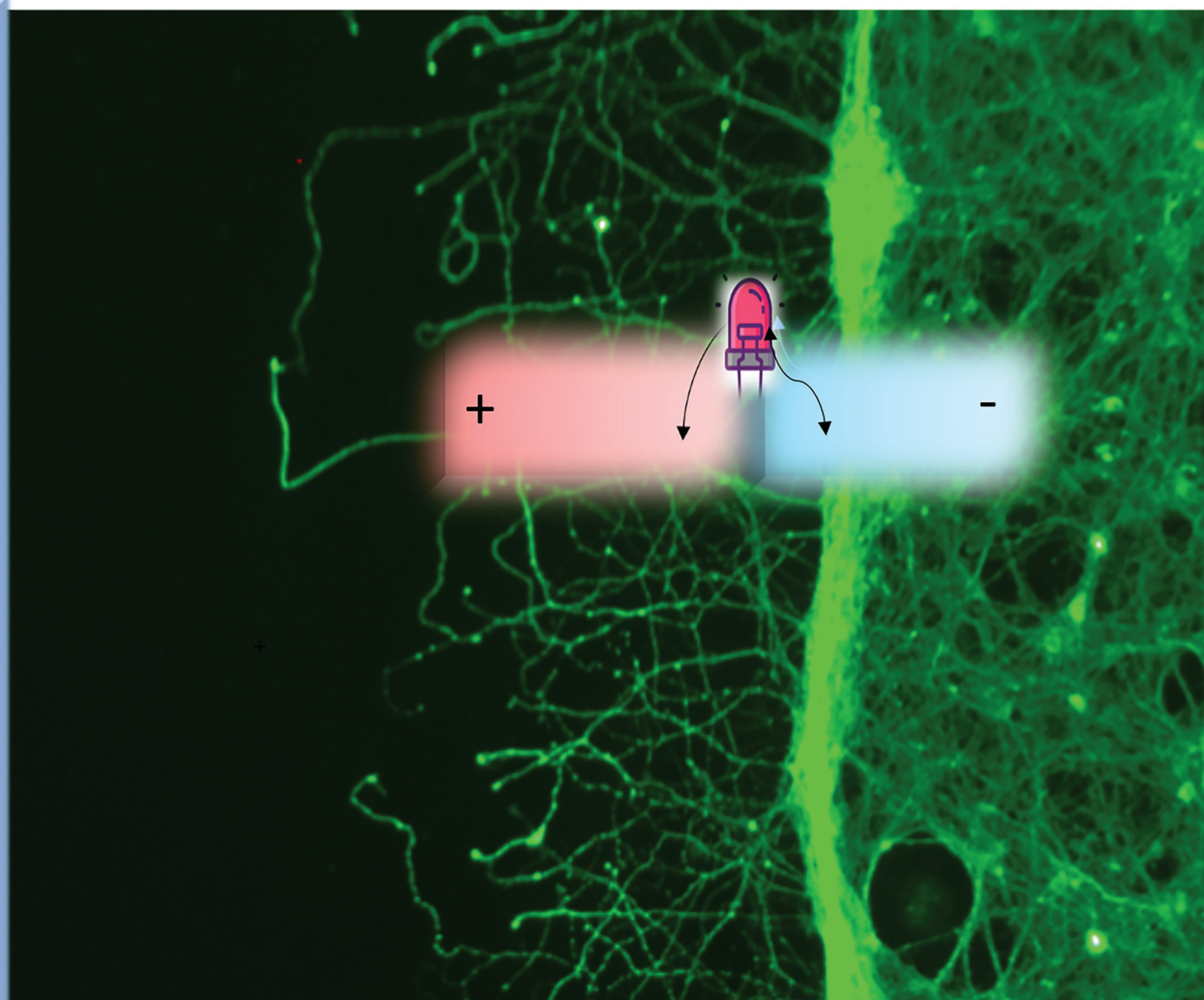


# Biomaterials Science

Volume 12  
Number 9  
7 May 2024  
Pages 2171-2450

rsc.li/biomaterials-science



ISSN 2047-4849

**PERSPECTIVE**

Ann M. Rajnicek and Nieves Casañ-Pastor  
Wireless control of nerve growth using bipolar  
electrodes: a new paradigm in electrostimulation



Cite this: *Biomater. Sci.*, 2024, **12**, 2180

## Wireless control of nerve growth using bipolar electrodes: a new paradigm in electrostimulation

Ann M. Rajnicek<sup>a</sup> and Nieves Casañ-Pastor \*<sup>b</sup>

Electrical activity underpins all life, but is most familiar in the nervous system, where long range electrical signalling is essential for function. When this is lost (e.g., traumatic injury) or it becomes inefficient (e.g., demyelination), the use of external fields can compensate for at least some functional deficits. However, its potential to also promote biological repair at the cell level is underplayed despite abundant *in vitro* evidence for control of neuron growth. This perspective article considers specifically the emerging possibility of achieving cell growth through the interaction of external electric fields using conducting materials as unwired bipolar electrodes, and without intending stimulation of neuron electrical activity to be the primary consequence. The use of a wireless method to create electrical interactions represents a paradigm shift and may allow new applications *in vivo* where physical wiring is not possible. Within that scheme of thought an evaluation of specific materials and their dynamic responses as bipolar unwired electrodes is summarized and correlated with changes in dynamic nerve growth during stimulation, suggesting possible future schemes to achieve neural growth using bipolar unwired electrodes with specific characteristics. This strategy emphasizes how nerve growth can be encouraged at injury sites wirelessly to induce repair, as opposed to implanting devices that may substitute the neural signals.

Received 29th November 2023,  
Accepted 6th February 2024

DOI: 10.1039/d3bm01946b

rsc.li/biomaterials-science

### Introduction

Electrical activity at the organism, tissue, single cell, and sub-cellular scales supports processes key to survival and proper function in animals, plants and microorganisms. Although electrical activity of the nervous system is familiar to most people, electrical signals are present in all cells and their clinical or experimental manipulation can therefore impinge on important signalling events, cell division, cell migration and other processes, including tissue repair.

Functional electrostimulation is being used clinically in the nervous system, where long range electrical signalling is essential for function. When this is lost (e.g., traumatic injury) or it becomes inefficient (e.g., demyelination), the use of external fields can compensate for at least some functional deficits, but its potential to also promote biological repair at the cell level is underplayed despite abundant *in vitro* evidence for its control of neuron growth.<sup>1–5</sup> Consequently, an exciting new field of electrostimulation technologies is emerging based on the possible interactions of electric fields (EF), electrode materials, and the nervous system,<sup>6,7</sup> opening also interdisciplinary research at the interface of materials science, modelling,

neuroscience, and electrochemistry. New technologies include systems that encompass electrical recording, sensing, functional electrostimulation, and attempts to stimulate nerve growth to repair nerve lesions.<sup>8–18</sup>

This perspective article considers specifically the emerging possibility of achieving cell growth through the interaction of external electric fields using conducting materials as unwired bipolar electrodes, and without intending stimulation of neuron electrical activity to be the primary consequence. The use of a wireless method to create electrical interactions represents a paradigm shift and may allow new applications *in vivo* where physical wiring is not possible. Within that scheme of thought an evaluation of specific materials and their dynamic responses as bipolar unwired electrodes is summarized and correlated with changes in dynamic nerve growth during stimulation, suggesting possible future schemes to achieve nerve growth using bipolar unwired electrodes. This strategy emphasizes how nerve growth can be encouraged at injury sites wirelessly to induce repair, as opposed to implanting devices that may substitute neural signals. This new approach also considers the significance of the resulting ionic and redox gradients created within the unwired electrode, the inherent oxidation state gradients and their electrochemistry, the related physical resistivity changes of the bipolar unwired electrode, changes in ionic gradients within the extracellular medium, and the medium impedance. Those factors may collectively influence the speed and direction of nerve growth and

<sup>a</sup>Institute of Medical Sciences, University of Aberdeen, Aberdeen, AB25 2ZD, Scotland, United Kingdom

<sup>b</sup>Institut de Ciència de Materials de Barcelona, CSIC, Campus UAB, 08193 Bellaterra, Barcelona, Spain. E-mail: nieves@icmab.es



other environmental factors, including inflammation. The inherent complex evolution of induced potentials and ionic and redox state gradients at the immersed unwired electrode would also impact cell growth, the local tissue microenvironment, and immunological responses, suggesting specific key points to be addressed in the future.

## Endogenous electric fields and injury currents in animal tissues

A basic principle in living systems (defined in electrophysiology) is the separation of charged ions across a resistive barrier (e.g., plasma membrane, organelle membrane). That is, a gradient of ion distribution in space (e.g., in cell cytoplasm or within extracellular spaces in tissues). Membrane potential describes the difference in electrical potential across the electrically resistive membrane and in excitable cells (e.g., neurons) a rapid wave-like change in potential (action potential) is the basis for electrical signal conduction. However, in

non-excitable cells membrane potentials also influence cell function. On a larger scale, stable voltage gradients in embryonic and adult tissues underpin a range of important events during development, tissue regeneration, cancer progression, and wound repair processes.<sup>19–23</sup>

The physiological basis for endogenous electrical signalling at the tissue level is best understood using frog skin as an example, but the same principles apply to any tightly sealed ion-transporting epithelium (Fig. 1A), including mammalian epithelia (e.g. cornea, gut lining, breast ducts, blood vessels, etc.). Asymmetric distribution of specific ion channels and pumps in the apical and basolateral membranes of cells in intact epithelial layers leads to net transport of charged ions across the structurally polarized cell layers, resulting in separation of charge across the highly resistive epithelium. For example, in frog skin  $\text{Na}^+$  moves inside cells passively through apical (facing the pond water) membrane sodium channels and it is then actively pumped out of the cells (to the extracellular spaces within the frog tissues) by the  $\text{Na}^+/\text{K}^+/\text{ATPase}$  pumps located in the basolateral membranes (facing the frog



**Ann M. Rajnicek**

*Dr Ann Rajnicek received her BS degree in 1984 from Marygrove College (USA), and her PhD degree in Developmental Biology from Purdue University (USA) in 1990. She is a Senior Lecturer at the University of Aberdeen (UK) with a long-standing research interest in electrical control of wound healing and nervous tissue repair in the context of spinal cord injury.*



**Nieves Casañ-Pastor**

*Prof. Casañ-Pastor graduated in Chemistry from the University of Valencia and had her PhD at Georgetown University (Washington DC, USA) in 1988. After a postdoc at the University of Valencia she got a permanent position as Researcher at the Institut of Materials Science of Barcelona (Spain) in 1990, where she is Research Professor since 2007. She has worked on mixed valence nanoclusters (polyoxometalate blues) and their magnetic properties when delocalized electrons are present. She has developed solid state electrochemical processes to intercalate oxygen in cuprates, manganates, yielding to room temperature transformation to superconductors, metals and ferromagnets. She has worked in electrodeposition of mixed metals for the development of  $\text{YBa}_2\text{Cu}_3\text{O}_7$ . During the last two decades she has been involved in the development of new hybrid materials based on iridium oxides, conducting polymers and nanocarbons to achieve large charge capacity biocompatible electrodes that facilitate neural growth minimizing radical formation. In the last stage she is developing wireless methods using bipolar electrochemistry for bioelectrodes and changes in physical properties. She has been leading a number of grants since 1990 involved with fundamental focussed electrochemistry, materials and bioelectrodes. She has been awarded several prizes along her career including a Volkswagen-CSIC and Marato Foundation TV3 prizes. She has also been a member of the CSIC Scientific Advisory Board, and of a number of Evaluation Panels from the Spanish Science Agency, and European Committees.*





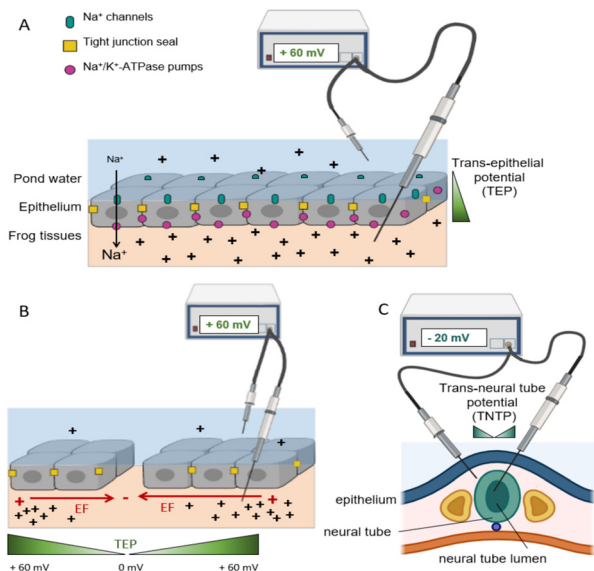


**Fig. 1** Structurally polarised epithelial cells, in which  $\text{Na}^+$  channels are restricted to apical cell membrane surfaces (pond water side) and the  $\text{Na}^+/\text{K}^+$ -ATPase pumps are localised to the basolateral cell membranes (frog tissue side). Neighbouring cells are fastened to each other by tight junctions, which provide a high resistance epithelial seal and they also aid physical segregation of ion pumps and channels in apical and basal membrane domains, respectively. Net inward movement of  $\text{Na}^+$  ions creates an internally positive transepithelial potential difference (TEP) relative to the pond water of about +60 mV. (B). Upon wounding, the  $\text{Na}^+$  ions leak out of the wound, collapsing the TEP to 0 mV at the injury, but distal to the wound (intact epithelium) the inward ion flow is uninterrupted, so the TEP remains +60 mV. The resulting potential difference between the wound site and intact tissues generates an electric field (red arrow) parallel to the epithelial layer, with the wound centre as a cathode (negative). The green wedge indicates the TEP gradient within tissues. (C) The embryonic neural tube, which is the precursor to the brain and spinal cord, maintains a potential difference of about -20 mV across itself. It forms from folds of the outer layer of the embryo, so its inside lumen shares ion transport traits with apical frog skin. Consequently, the lumen is negative relative to the tissues just outside the neural tube. Extracted from ref. 3 under Creative Commons License.

tissues). The  $\text{Na}^+$  ions do not leak out due to the tight junctions that connect neighbouring cells, creating a tight barrier seal. Consequently, there is an imbalance of charge across the epithelial layers, with more positive charges at the inside of the frog's skin relative to the pond water. This inwardly positive transepithelial potential (TEP) across the skin is  $\sim +60$  mV in frog, and similar values (on the order of tens of mV) have been recorded in mammalian epithelia.<sup>23–27</sup>

The TEP is steady until the integrity of the epithelial layer is compromised. Upon epithelial damage the  $\text{Na}^+$  ions that have accumulated beneath the epithelium immediately start to leak out the low resistance wound, but in distal regions the normal inward  $\text{Na}^+$  transport continues. Therefore, the TEP at the wound falls catastrophically to 0 mV but the normal +60 mV TEP persists distally (Fig. 1B). The difference in voltage (TEP) over distance is, by definition, an electric field. Therefore, the wound creates a natural electric field in the tissues just

beneath the epithelium (directed parallel to the epithelium). It is on the order of hundreds of  $\text{mV mm}^{-1}$  immediately adjacent to the wound margins, its magnitude falling exponentially with distance from the wound. In this scenario the centre of the wound, where  $\text{Na}^+$  ions are leaking out, is relatively negative (cathode) compared to distal areas where polarized  $\text{Na}^+$  ion transport is undisturbed (anode).

In such biological systems the direction of current flow is conventionally considered to be the direction of movement of positively charged ions. Therefore, the wound has both a natural outward injury current (mainly due to leakage of  $\text{Na}^+$  ions out of the wound) and a correlated electric field arising from the internal voltage gradient (parallel to the epithelium in tissues adjacent to the wound). Significantly, the electric field and injury current have roles in facilitating natural wound healing and this recognition has led to established clinical therapies to aid healing using electrical stimulation.<sup>28,29</sup>

Injury potentials and currents are always associated with damaged tissues that exhibit regenerative capacity, including amputated amphibian limbs, tadpole tails, zebra fish tails, and juvenile human fingertips.<sup>23,30–33</sup> Naturally occurring electrical gradients are also present near the uninjured embryonic amphibian brain and spinal cord (Fig. 1C), suggesting putative roles in nervous system development.<sup>34–37</sup> For example, the central nervous system emerges in embryos as an upfolding of parallel ridges of specialised epithelium along the dorsal midline that fuse to form a distinct hollow tube, the neural tube (Fig. 1C). The entire embryonic central nervous system therefore shares the skin's epithelial barrier and ion transport properties, including a *trans* neural tube potential difference of about 20 mV between the inner lumen (relatively negative) and the tissues just outside of the neural tube.<sup>34,35</sup> Consequently, central nervous system neurons are born into and extend axons within a naturally occurring electric field in the neural tube, which in *Xenopus laevis* frog exceeds  $400 \text{ mV mm}^{-1}$ .<sup>34,36</sup>

In the context of nervous system damage, injury currents (ion flow around sites of damage) have been measured near the damaged lamprey and adult mammalian spinal cords.<sup>37,38</sup> It follows therefore that electric fields imposed through external electrodes could potentially modify cell function and behaviour, including the rate and direction of nerve growth in ways that could stimulate nerve connectivity and tissue repair.<sup>2–5,18,39,40</sup>

How do extracellular electric fields impact cell function? In the context of healing, externally applied electric fields of a magnitude similar to those measured in tissues (physiological electric fields) impact many significant physiological events, including gene expression, immune function, phagocytosis, tissue regeneration, and embryonic development.<sup>3,23,40–43</sup> However, some clinical therapies for the nervous system use much higher stimulation amplitudes (non-physiological), where the applied field near the implanted electrodes may be large enough to impact neuronal firing and synapse function. This concept has been leveraged to manage symptoms for diverse neurological diseases including Parkinson's, depression, epilepsy, and migraine.<sup>43,44–51</sup> It may also be the basis for other recent applications in which implanted elec-



trode arrays were used to effectively bypass damaged spinal cord regions to overcome functional deficits in clinically functionally complete (total loss of sensory and motor function below the injury) spinal injured patients.<sup>44–47</sup>

Although the fundamental mechanisms of the interaction between cells and electrodes are not fully known, some common factors emerge. For example, extracellular ionic gradients (Fig. 1) influence cell behaviour. Sufficiently large extracellular potentials can alter a cell's membrane potential or influence the threshold required for firing action potentials, but smaller, physiological scale potentials steer neuron growth cone direction and branching, direct migration of neurons, control neural stem cell fates, control glial cell orientation and behaviour, and influence immune and inflammatory mechanisms.<sup>2,4,47,52–55</sup> Furthermore, when an injury has occurred, the existence of new endogenous directional fields suggests that regeneration may be enhanced with the help of external fields that modify scar tissue. Implanted materials used to apply larger potentials always have a foreign body response, inducing inflammation and fast encapsulation, which results in an enhanced impedance. Consequently, sensing or actuating becomes partially hindered, necessitating removal or replacement of the electrode after several months.

## Electrode materials and electrostimulation protocols

Most studies of nerve cell responses to exogenous electric fields have used direct current (DC) stimulation because the endogenous injury currents and wound associated electric fields are DC in character (Fig. 1). However, alternating current (AC) fields can occur naturally (*e.g.*, nerve synapse potentials) and when applied exogenously they impact nerve cell function and axon sprouting.<sup>53</sup> The responsiveness of nerve cells to AC fields has led to clinical electrostimulation protocols using AC fields with zero net charge (balanced polarity and intensity when averaged over the cycle) and oscillation frequencies determined empirically. These conditions attempt to minimize tissue damage through net zero delivered charge.

Some studies used slowly oscillating square wave AC pulses (15–30 min long cycle periods, balanced polarity and intensity over short and long-time spans) delivered using Pt/Ir wires intended to stimulate growth of both sensory and motor nerve pathways in the spinal cord.<sup>18,55–60</sup> Studies using *in vitro* scratch models and new materials with large charge capacities based on iridium oxide (IrOx), IrOx–nanocarbon hybrids, and conducting polymers with amino acid counterions<sup>61</sup> used pulsed DC fields, or AC net charge protocols over short time periods resulting in enhanced repair in both sides of the scratch, but not when Pt electrodes were used. However, AC stimulation (~300 Hz) is used more often to restore function by acting on spared nerve pathways which may include central pattern generators.<sup>45–47</sup> Intriguingly, when using AC stimulation, the improvement depends on the continued presence of the stimulus rather than affecting a chronic improvement. For example,

functional recovery (*e.g.*, supporting body weight in a static standing position, or volitional ankle flex) is lost when the AC stimulation is stopped.<sup>45–47</sup> A similar response was observed for AC lumbar spinal stimulation to facilitate gait in Parkinson's.<sup>62</sup> Therefore, the specific combination of protocol and electrode material defines the outcome of electrostimulation, with DC schemes seeming to favour cell growth and repair.

Regardless of the desired electrostimulation method, fundamental aspects of electrochemistry must be considered because electrodes are inevitably immersed in a biological ionic fluid. Thus, capacitive and faradaic effects exist, and specific limits must be considered. Steady, long-term DC (no change in polarity) stimulation is unattractive if the charge capacity of the electrode is surpassed, due to the generation of undesirable electrode effects, such as localised pH changes, heat production and generation of free radical species that are detrimental to surrounding cells and tissues.<sup>9,10,63</sup> Therefore, ideal parameters would deliver current or charge minimizing such undesired chemical reactions, ideally using large capacity electrodes.

Even state of the art clinical work has used electrodes hard-wired to an external power source, with materials derived from fundamental engineering principles. Indeed, in some cases little attention is given to the electrode material and sometimes it is not even specified in publications. Most electrodes used clinically are only capacitive in nature (*e.g.*, Pt, PtIr, stainless steel, or titanium nitride (TiN)) delivering a small amount of charge in each pulse.<sup>9,10</sup> Nonetheless, they are often adequate for the intended purpose. A problem recognised by neurosurgeons using existing implanted electrode materials is inflammation and encapsulation, which eventually necessitates electrode removal or replacement as performance decays. Therefore, there is an urgent need for improved electrode materials and protocols.

As mentioned above, electric field protocols used clinically to modulate functional symptoms in the nervous system try to compensate globally the charge delivered to the biological system by using AC fields with net zero charge.<sup>9,10</sup> Electrical stimulation for Parkinson or depression is done with typical DBS parameter settings for movement disorders ranging from 2 to 4 V (mm range) amplitude, 60–450  $\mu$ s pulse width, 130–185 Hz frequency.<sup>64</sup> Charge delivery from electrode to the electrolyte is thus controlled only based on the interplay of the capacitive and faradaic charge delivered to the electrolyte by adjusting current and frequency of oscillation.<sup>64</sup> However, short time scale reactions of O<sub>2</sub> and H<sub>2</sub>O yielding reactive oxygen radicals are difficult to avoid if the electrodes do not assume the charge transfer, as is the case for capacitive metal electrodes. And only by modulating the electrode material properties may the charge transfer mechanism be switched out of the bulk electrolyte.

## Electrode materials and charge capacities

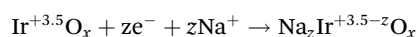
A number of *in vitro* studies using different substrate materials, including those with different topographies, and



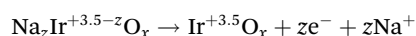
insulating or conducting properties, have revealed clear candidate materials, whilst highlighting how little is known about the mechanisms of interaction of electrodes, materials, cells, and biological media.<sup>65–74</sup> Obviously, direct contact electrodes must be sufficiently conducting, and the charge transfer between the electron conducting electrode and the ionic conducting medium is a key factor in the success or failure of the EF application. As mentioned, charge transfer at the electrode-cellular medium interphase is unsafe if the electrolyte assumes the charge, since it involves secondary reactions related to the production of reactive oxygen species due to water oxidation and O<sub>2</sub> reduction. Capacitive aspects on the other hand are known to induce heating and tissue damage. Thus, cell culture experiments are performed using salt bridges at the electrodes to isolate cells from electrode reaction products, or by using adhesion layers such as collagen, which provide physiological cell attachment, but they also separate cells physically from the electrode material. Clinical *in vivo* protocols on the other hand, cannot use salt bridges, instead they minimize damage during electric field application using very short pulse stimulation times in AC mode, within frequencies that minimize damage for the electrodes used. Indeed, if inert electrodes like Pt or other noble metals are used the charge transfer must occur at the ionic liquid near the electrode surface. *In vitro* cell culture shows however, that short term stimulation processes with DC and net charge that when using Pt electrodes, both water oxidation and O<sub>2</sub> reduction processes occur for very low charge injected (in the order of 100 μC cm<sup>-2</sup>). Specifically, cathodic O<sub>2</sub> reduction yields species more toxic than those from water oxidation.<sup>61</sup> There is also evidence that the species released by platinum or steel metal species are cytotoxic.<sup>61,65,66,75</sup>

Thus, materials that undergo charge transfer within their inner structure, thanks to the mixed ionic-electronic conductivity, may be considered optimal. This is because the material is able to undergo redox chemical process in which the electron is transferred into a mixed valence charge state simultaneous with the ionic intercalation/deintercalation process, thus eliminating the need of the electrolyte reactions. If that occurs in a specific material within the potential window of aqueous solutions, it greatly enhances the charge capacity limits imposed by the electrode material. A clear example is the pioneering use of coatings of IrOx tested,<sup>76,77</sup> that lower the electrode impedance. Since IrOx is actually an oxohydroxide, typical reactions involved under electrostimulation may be summarized as:<sup>77</sup>

Reduction:



Oxidation:



Since Na<sup>+</sup> intercalation has been observed in it,<sup>77</sup> (while K<sup>+</sup> initially occluded in the structure is removed upon sterilization).

Equivalent intercalation reactions also happen in the case of PEDOT-PSS (poly(3,4-ethylenedioxythiophene)-poly(estyrene

sulfonate)) and other conducting polymers, always simultaneously to a change in oxidation state or charge carriers within the polymer. Remarkably both types of compounds are oxidized and offer an initial redox behaviour upon reduction.

New materials fulfilling biocompatibility criteria, even in the presence of electric fields, are appearing in the global electrode scenario. They are mostly based on iridium oxide, carbon nanomaterials (nanotubes and graphenes, sometimes in 3D form) and conducting polymers, in bulk and coating forms, as well as the hybrid materials related to them, IrOx-carbon nanotubes, IrOx-graphene, and IrOx-nanocarbons-conducting polymers.<sup>65–75,77</sup> Thus, as previously proposed,<sup>59,63,64,75</sup> using mixed valence intercalation materials as electrodes, able to intercalate ions and undergo mixed valence changes, the charge transfer is greatly enhanced up to two orders of magnitude with respect to Pt (μC cm<sup>-2</sup>), and improved neural repair is observed.<sup>66</sup> In that sense IrOx has been shown to achieve charge capacities in the order of 5 mC cm<sup>-2</sup>,<sup>77</sup> while conducting polymers like PEDOT-PSS reach 10 mC cm<sup>-2</sup>.<sup>78</sup> Multilayer coatings, like polypyrrole coating of PEDOT polymers, also show better biocompatibility especially when bioactive aminoacids (*e.g.* lysine) are used,<sup>78</sup> in which case PEDOT gives polypyrrole more resistance to oxidation in atmospheric conditions. Hybrid phases containing IrOx and nanocarbons reach 120 mC cm<sup>-2</sup>,<sup>65–67</sup> while hybrids containing iridium oxide, nanocarbons but also conducting polymers result in a nanostructure that involves the polymer encapsulating IrOx and carbon nanocomponents. The final charge capacity is only that of the polymer, near 10 mC cm<sup>-2</sup>. Such charge capacity limits define the cathodic charge that can be delivered during the constant DC potential range used. Additionally, since the inner solid state reactions behind the charge capacity are related to reversible redox intercalation processes as defined below, the new materials offer a whole range of action not possible until now.<sup>61,65,66</sup>

### Micro and nanostructures

3D structures that enhance the active surface are expected to increment the charge capacity. Both carbon and platinum black have been tested in cell growth experiments but few experiments with electric field application have been reported.<sup>79</sup> Topographic cues have also been demonstrated to influence neuron growth when using insulating substrates,<sup>80,81</sup> and very recently on nanostructured PEDOT-PSS in presence of EF facilitating directionality of growth.<sup>82</sup>

## Directionality in repair studies. Neuron growth using directly connected electrodes

Beyond the AC alternating field EF protocols used in functional electrostimulation with zero net charge, DC fields may also be used. A constant field direction (DC) results in induced directional ionic gradients in the extracellular and intracellular





matrix, which are relevant in tissue growth and embryo development,<sup>1–4</sup> as shown previously, inducing cell differentiation and growth but also major changes in development from original embryos. EF protocols using the new electrode types (IrOx hybrids and conducting polymers with biologic counterions) with sustained directionality and small application times (40 min pulsed DC) demonstrated effects on mammalian nerve cell outgrowth in a scratch wound assay.<sup>61</sup> In those experiments, the effect depends on the electrode used and its chemistry; capacitive Pt electrodes impaired healing compared to the spontaneous healing observed in controls.<sup>61</sup> On the other hand, in the presence of EF stimulation both sides of the scratch wound edge advanced toward the lesion center, regardless of whether facing the anode or the cathode.<sup>61</sup>

In all cases mentioned above the electrodes were wired directly to an external programmed power source with a logic scheme for easy control of applied current, voltage, and pulse time. However, a substantial serious drawback in electrostimulation protocols aimed to enhance function or repair is the need to wire the implanted electrode to external power sources, or to an inserted stimulator unit (*e.g.*, deep brain electrostimulation<sup>9</sup>).

## New wireless approaches based on bipolar electrochemical induction

Although a number of wireless approaches are being pursued, including piezoelectric, and light effects,<sup>83,84</sup> the closest approach to a connected electrode is an unwired electrode where polarization may induce charge transfer in the same fundamental basis and electrochemical paths tested on connected electrodes.

Attempts have been made to create local microbatteries by placing power sources directly onto wounded tissues. For example, materials patterned with alternating dots of Ag and Zn have been used on skin tissue treatments<sup>85,86</sup> but those reactive systems that may lead to batteries are not biocompatible and cannot be implanted without substantial damage to the local tissue. Metamaterials formed by a composition of spatially organized materials with diverse properties may lead to a self-rectifying implantable device where current may be induced in a single direction through an external magnetic field,<sup>87</sup> offering big potential despite the complexity of the acting implant.

Recent experiments have shown that an unwired bipolar electrode can be generated *in vitro* through induction of polarization in an immersed conducting material, yielding wireless bipolar electrochemistry effects on neurons.<sup>88</sup> This pioneering work showed that wireless electrostimulation was possible through the induction of dipoles at the borders of immersed conducting materials in the presence of externally imposed electric fields and that neural growth parameters were affected without direct wiring to a power source. Significantly, these experiments are also the basis that sustain the newly rectifier device<sup>88</sup> or any other where the electric field may be generated by an oscillating magnetic field.

It was demonstrated that *Xenopus laevis* neurons isolated from the embryonic neural tube growing directly on conducting materials underwent significant neurite outgrowth compared with those grown on insulating materials<sup>88</sup> and that

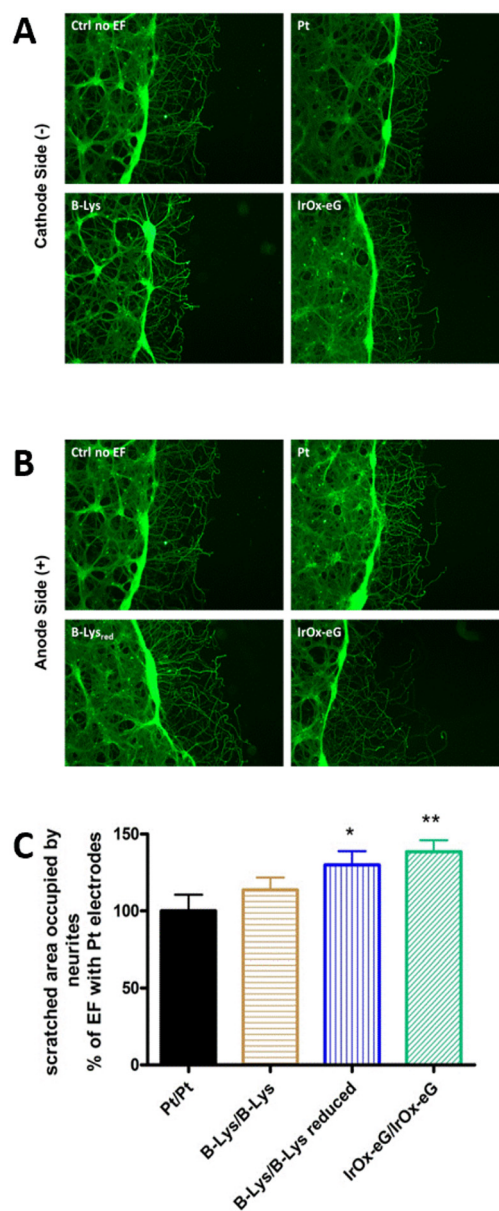


**Fig. 2** Wound closure in a cortical scratch wound assay. (A) and (B) Fluorescence micrographs of Tau immunostaining. The dark region to the right is the scratch. Neurites extended spontaneously into the scratch region. In the presence of EF using various electrodes: uncoated Pt, bilayer PEDOT–polypyrrole–lysine coating platinum, with Q delivered 80% of the cathodic charge capacities (CSC) values, and IrOx–graphene coating Pt electrode with equal Q delivered: (A) cathode side and (B) anode side. (C) Wound closure in a cortical neuron scratch model using PEDOT–polypyrrole–lysine coatings and IrOx–graphene coatings using max 40 min stimulation with charge delivery below the maximum charge capacity of the lower capacity material. Note: as the charge capacity is enhanced in the material (conducting polymer reduced, or IrOx–graphene), the repair for a certain Q is larger. Reproduced from ref. 61 with permission from Elsevier, copyright 2017.



bipolar effects were evident in the materials (Fig. 4). Electrostimulation effects on cells were observed using much lower fields ( $50 \text{ mV mm}^{-1}$ ) than those traditionally used for insulating materials assays ( $\sim 150 \text{ mV mm}^{-1}$ ) or other insulating biocompatible substrates such as  $\text{TiO}_2$  or glass, evidencing a wireless electrical influence that has been explained and proven in consecutive publications.<sup>88–93</sup>

*Xenopus* neuron cultures offer several advantages over mammalian neurons for these experiments, permitting a clearer interpretation of the effect of the wireless bipolar electrodes on neuron growth. First, mammalian neurons *in vitro* typically require an adhesion layer for cell attachment and to support neurite outgrowth but *Xenopus* neurons grow directly on the uncoated material surface. This provides unimpeded, intimate contact of the growth cone with the underlying material, so any changes in the material properties resulting from an imposed field are sensed directly by the cells and are reflected in changes in cell growth. Additionally, *Xenopus* neurite growth cones are significantly larger in diameter, and their neurites extend much more rapidly than those on mammalian neurons. In a practical sense it is also much easier to control experimental conditions because no additional growth factors are required for *Xenopus* cultures, and only 1% calf serum supplementation is required, which contrasts to a complex growth factor cocktail and the addition of 10% serum for mammalian neurons, facilitating time lapse observations. The low protein content minimizes possible protein adsorption to electrode materials. Finally, time lapse observations are readily achievable on *Xenopus* neurons since they grow in ambient temperature and  $\text{CO}_2$  conditions, so no incubator is required. Thus, the experiments are reduced to the simplest, controllable elements that permit correlation of cell behaviour with changes in material properties.

While induced bipolar electrochemistry effects had been known previously, only recently have they been made more visible.<sup>94–104</sup> The essence of the effect requires a conducting material to be immersed within the electrolyte, which undergoes an induced polarization (opposing the externally imposed

field). Such polarization results in spatially opposed induced anode and cathode parts, where reactions may occur at the electrolyte–bipolar electrode interface, thus having electrochemistry without the need of wiring the electrode. Fig. 3 illustrates a scheme of the voltage profile induced when a conducting material is immersed in the electrolyte, and the actual voltages deviation at the material Poles that become the induced cathode and anode. It is actually the deviation from the electrolyte potential profile what we deal with when we speak of induced potentials. Furthermore, when induced potential are mentioned it refers to the potential profile induced in the

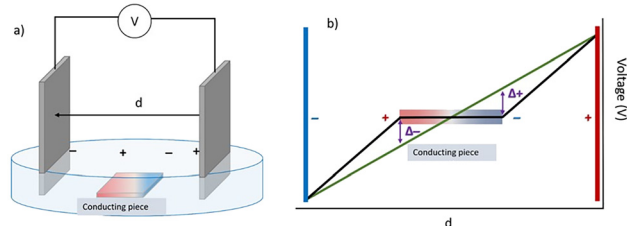


**Fig. 3** Polarization induced on a conducting material immersed in an electrolyte. (a) Scheme of an electrochemical cell with an immersed conducting material and (b) the resulting potential profile in absence and in presence of such material. In b, the red and blue lines represent the external positive and negative wired electrodes, while the horizontal charged material is the bipolar electrode. The induced potentials  $\Delta+$  and  $\Delta-$  depend on the distance between external electrodes,  $d$ , and the actual length of the bipolar unwired electrode,  $l$ , as expected from classical electromagnetism rules, as well as the position of the material within the field lines. Reproduced from ref. 91 with permission from ECS (IOP publisher), copyright 2022.

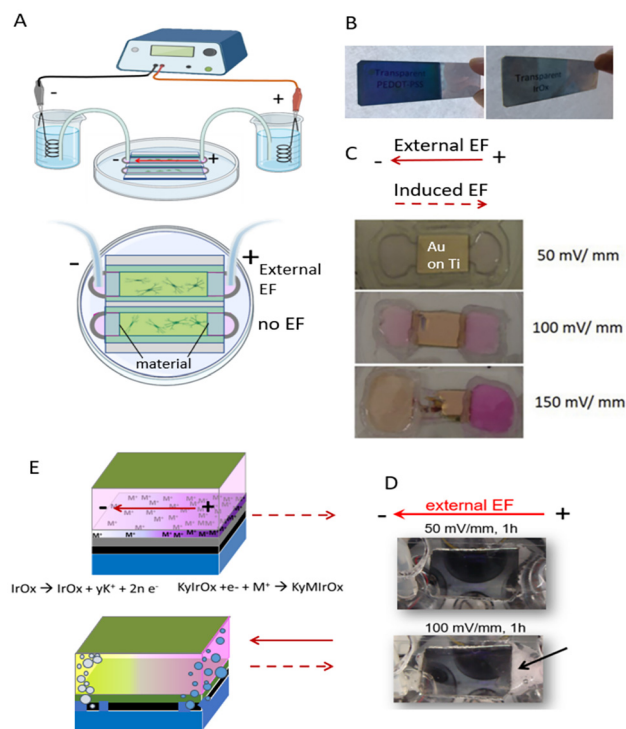


**Fig. 4** Establishing bipolar conditions in cell cultures: (A) electric field apparatus. (B) Glass microscope slides coated with PEDOT–PSS (top) and IrOx (bottom) demonstrating transparency. (C) When the material used was gold coated onto a titanium adhesion layer (on glass slide) the phenol red pH indicator in the cell culture medium proved a gradient of pH developed as a consequence of the electric field (external cathode is at the left). Phenol red is yellow under acidic conditions and is pink at alkaline conditions. A pH gradient exists at EFs  $\geq 100 \text{ mV mm}^{-1}$  because at the higher potentials  $\text{H}_2\text{O}$  oxidizes to  $\text{O}_2$  at the induced anode, leaving additional  $\text{H}^+$  and therefore lowering pH. Conversely, at the induced cathode  $\text{H}_2\text{O}$  reduces to  $\text{H}_2$  leaving  $\text{OH}^-$  behind, thus raising the pH. (D) Bubbles emerge at the extreme ends of the materials (both induced Poles) at high potentials, suggesting such gas production occurs. (E) Scheme for inducing polarity in the conductive materials at high and low potentials. Gas is produced at both induced Poles in materials under  $150 \text{ mV mm}^{-1}$  conditions; glass/Ti/Au multilayer behaviour at 50, 100 and  $150 \text{ mV mm}^{-1}$ . Detachment of the 5 nm Ti underlayer (black layer) used for better adhesion of gold (orange layer) is observed at  $150 \text{ mV mm}^{-1}$ , due to oxidation of Ti underlayer to  $\text{TiO}_2$  at the induced anode. At  $50 \text{ mV mm}^{-1}$ ,  $\text{Na}^+$  ions intercalate at the induced cathode pole for materials allowing it like IrOx and PEDOT–PSS. IrOx intercalation has been shown with  $\text{K}^+$  originally embedded in the structure. Reproduced from ref. 88 with permission from Wiley, copyright 2018.





material, as opposed to the potential profile present in the electrolyte (which would match the external EF polarity). Therefore, the induced potential and the direct potential in the electrolyte have opposite polarities (anode and cathode).

Although the effect is usually seen on metals, small gap semiconductors like iridium oxides or conducting polymers also show it.<sup>89,90,103</sup> The magnitude of the conductivity required in the material, with respect to the electrolyte conductivity, is the relevant factor as has been studied recently.<sup>93</sup> The induced potentials will change depending on the imposed external potential and the distance between the external electrodes. The reactions occurring at the induced Poles will depend on the induced potentials, as would occur with a connected electrode. Furthermore, because ionic conductivity exists in such materials, the pole is not confined to the extreme ends of the conducting material and a voltage profile exists across the immersed piece (represented in Fig. 3 as red and blue zones for positive and negative induced charges). In turn, the gradient in potential generates a gradient in redox state and intercalated ions or composition that may be optically visible, since colour depends on oxidation state. That has been studied recently using local resolution techniques described below, evidencing the large complexity that is possible for each specific material.

## Wireless bipolar conditions impact neuron growth

When experiments with cell cultures are performed in such systems in the presence of an external electric field (see Fig. 3 and 4), the cells may be sensitive to the polarization of the immersed conducting material, and to all the effects that the polarization causes, as we discuss below. For *Xenopus* neurons 150 mV mm<sup>-1</sup> is used typically as the imposed external field with insulating substrates because it is in the physiological range. However, when a conducting material is used in presence of a pH indicator the effect of the induced field can be easily observed through the formation of H<sub>2</sub> and O<sub>2</sub> bubbles at the induced cathode and anode, respectively at fields 100 mV mm<sup>-1</sup> and above (Fig. 4). On the right in Fig. 4 the negatively induced pole forms H<sub>2</sub> and OH<sup>-</sup> at high potentials, and the pH indicator turns to its pink basic form. This specific detail enabled a selection of a more appropriate applied field to prevent water side reactions during neuron growth experiments. Significantly, the final studied field, 50 mV mm<sup>-1</sup> is a third of the field intensity usually used for insulating substrates, and as shown later, the effects would be much larger on neuron growth.

In such work,<sup>88</sup> the conducting materials tested included coatings of noble metals, like Au and Pt, and complex mixed-conducting mixed-valence intercalation systems like IrOx, or conducting polymers, like polypyrrole-X or PEDOT-X (with X being the counteranion to the positively charged polymer) and related systems. Initial tests allowed a selection of materials that supported neuronal growth and cell growth was then compared with materials like insulating culture glass or TiO<sub>2</sub>. In

many cases, cell growth was supported better than on standard insulating tissue culture glass. Under the external electric field, the neuron response was specific for each material. The speed of neurite growth was faster on some conducting materials, while the extent (angle) of neurite growth toward the external driving cathode was more clearly defined on some other conducting material types, suggesting that an internal material chemistry was affecting the behavioural outcome. A range of potentials in which intercalation does occur exists within the window of potentials for water evolution.

When neurites exhibited directional turning it was consistently towards the external driving cathode, regardless of material, implying that the electrolyte ionic gradient may dominate over the ionic gradient due to intercalation in the material. It would be desirable to analyse further how both types of co-existing ionic gradients, which in principle oppose each other (see below), may interact to control neurite growth. On the other hand, the degree of capacitive vs. faradaic charge capacity in each of the cases is only now starting to be envisaged, as shown by the studies described below.

Importantly, the influence of the field on cell growth and the angle of neurite turning were larger, even when using electric fields much smaller (50 mV mm<sup>-1</sup>) than those used previously (150 mV mm<sup>-1</sup>) on insulating glass or plastic substrates. All of them behave in the same range of potential as the Au coating shown (Fig. 5).

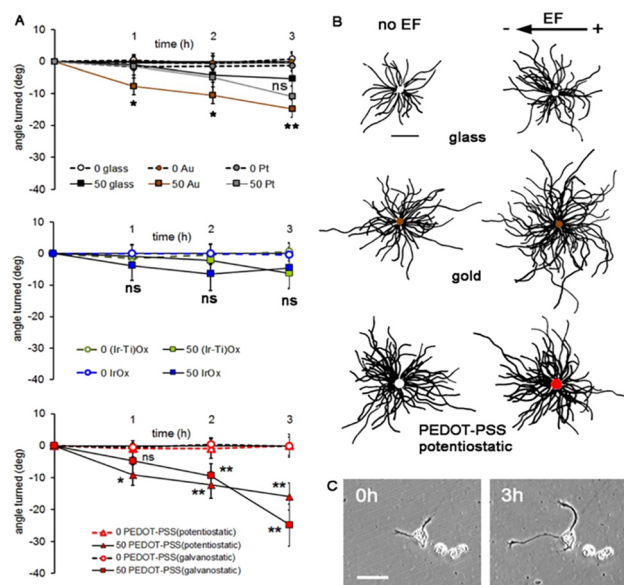


**Fig. 5** Neuron growth during 50 mV mm<sup>-1</sup> external electric field (EF) stimulation. (A) The angle of growth cone migration. Negative values indicate migration toward the external cathode; zero indicates randomly directed migration. Statistics compared to the same substrates but without an EF (Student's 2-tailed t-test). \**p* ≤ 0.05, \*\**p* ≤ 0.005, and ns = no significant difference. (B) Composite drawings made by superimposing the cell bodies and tracing each neurite. Scale 100 μm. The electric field vector represents the external field imposed within the culture medium. (C) A neuron growing on PEDOT-PSS (galvanostatic). Scale 50 μm. Reproduced from ref. 88 with permission from Wiley, copyright 2018.



The bipolar charging effect depends on the size of the metal immersed in a first simple approach, as mentioned before. It can occur at small scales including nanoparticles, as it has been found in very thin layers (50 nm of cobalt nitride, CoN, on Au),<sup>105</sup> in Janus particles, Au nanoparticles<sup>106,107</sup> and others.<sup>103</sup> Thus, previous work reported using coatings of gold nanoparticles where neurite outgrowth was observed under EF conditions may now be considered using in a new perspective.<sup>105</sup> Although no data for possible electronic percolation had been extracted it can be assumed that in such work the bipolar effect was also acting through polarization of the gold nanoparticles.

Two years after our observations of bipolar effects on neurons, there was independent confirmation of wireless bipolar electrochemistry effects on neural growth using a rat cell line (PC12) that can be driven to a sympathetic neuron like phenotype. The study showed that the extent of proliferation and the number and length of neurite processes were enhanced on conducting polypyrrole polymers when using DC external electrode system conditions that would induce bipolar effects in the material.<sup>108</sup> However, that study incorporated collagen into the underlying material, so does not permit the advantage of direct material–neuron interface offered by our *Xenopus* model system (Fig. 6).

**New therapies based on bipolar electrochemistry** are emerging that extend beyond control of nerve cell growth. A recent parallel study presented an alternative point of view of bipolar electrochemistry applications in cells. Electrical polarization induced in functionalized gold nanoparticles within cells may yield an anti-cancer treatment to target glioblastoma.<sup>106</sup> When

Au nanoparticles are functionalized with redox available agents which are biologically active, under external AC electric fields, the redox reactions derived from induced bipolar electrochemistry at the Poles of gold nanoparticles, yield a significant anticancer effect.<sup>106</sup>

It is interesting that the effect occurs despite the use of AC stimulation because it would induce alternating polarization in the Au nanoparticles, and despite the movement of the freely suspended nanoparticles within the cell, which would also induce a random polarization of the particles (as opposed to those fixed to a surface). Although no evidence was provided in terms of effects on cell migration or growth, the phenomenon is significant and suggests the need for additional studies in the field. In support of this notion, highly asymmetric carbon nanotubes have also been shown to induce significant polarizations in biological cases.<sup>109</sup> In particular, the use of AC pulses in both cases suggests possible polarization dynamics that must be investigated further.

As bipolar electrodes used in those therapies may reach the small size of nanoparticles, these technologies encompass the new concept of electroceuticals, innovative tools that use electrical strategies to influence physiology with consequences that may resemble actions of pharmaceuticals. However, specific configurations for the external driving electrodes are still needed to drive this exciting new discipline forward. We suggest that electrostimulation using wireless induced bipolar electrochemistry involves a new paradigm by which biological systems may be actuated electroceutically, opening a new route for clinical electrical therapies without the need for direct wiring at the specific location of the electrode. The consequent physiological responses may impact fields like drug delivery, functional electrostimulation, repair electrostimulation, or interfaces for sensing applications.

Remarkably, additional experiments have shown that an external imposed field may not be required to observe the bipolar effect on implanted biosystems. Living cells create an environment with endogenous electric fields that may induce local charging of the conducting material surface, which in turn may affect back the cell behaviour. A new vision of the possible interactions between the electrode material and the biological system therefore emerges through simple implantation of a conducting material, even without external electrodes connected to an external power source. For example, implantation of a conducting material *in vivo* (DBS) had significant effects on depression treatment in a rat model<sup>110</sup> while the implantation of an insulating material did not. Although many other variables are involved the study suggests that neurons generate a dynamic bipolar induction on the conducting material implanted. The resulting polarization of the material may impact neuron activity, creating a feedback loop interaction between the implant and the neural network.<sup>110</sup> This could indeed open new possibilities in terms of the new mechanism of action for electroceuticals, even in the absence of an externally imposed EF.

Interestingly, the effects of graphene layers on neural growth<sup>73</sup> or of conducting polymers on cardiomyocytes<sup>111</sup>

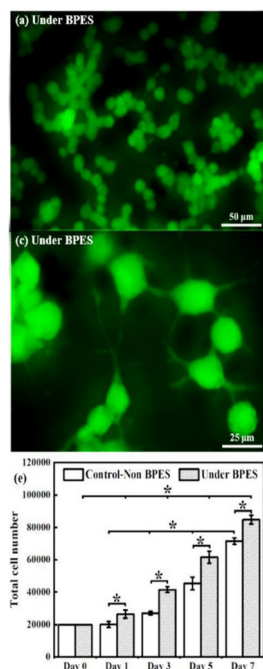


**Fig. 6** PC12 neurite development on polypyrrole polymers without and with bipolar effects when using a collagen adhesion layer. Reproduced from ref. 108 with permission from Elsevier, copyright 2020.



could be explained, in our opinion, on the same basis if cardiac cells generate polarization of the conducting material. Therefore, a deeper study is desirable regarding the existence of bipolar effects on implanted conducting materials, even revisiting the effects of materials reported in the past with and without active stimulation using an external source.

## Correlating conducting material bipolar effects, electrochemistry, and neuron growth

Among the possible physicochemical effects affecting neural cells in the wireless configuration of electrode materials, several crucial aspects have been studied to advance on the implications of wireless electrostimulation.

Beyond the ionic gradients known to exist in the liquid extracellular medium in the presence of electric fields, additional observations have been made on the non-biological part of the global system material–neuron environment summarized in three points:

(a) Evidence for the existence of a chemical gradient at the material acting as bipolar unwired electrode, and the dynamic character of such a gradient in chemical terms.<sup>89,91,104</sup>

(b) A corresponding gradient in the physical electrical resistance of the bipolar electrode correlated with the chemical gradient,<sup>93</sup> therefore changing the bipolar effect over time in some cases (*e.g.*, IrOx).

(c) A change in the global impedance when unwired electrodes are immersed.<sup>91,93</sup>

Each of those factors, or any combination of them, may influence cell growth and the environment in which neurons grow. Depending on the electrode material the resistance changes at the bipolar electrode in unwired conditions, possibly affecting the interface with neurons grown in the vicinity, removing part of the induction effect, or creating oscillation of the induced potential.<sup>92,93</sup> On the other hand, ionic gradients within the material and redox states may generate specific cues to which neurons are sensitive. Beyond the material itself, the extracellular medium is observed to have lower impedance when a bipolar conducting material is present, even at very low potentials (*e.g.*, when 10 mV perturbation is used for measurement).<sup>91</sup> These observations help pinpoint the fundamental physical and chemical aspects through which cells may interact with implants and also how cell growth may be influenced through induced wireless electrostimulation.

Above a certain conductivity of the material implanted, the polarization attained for various materials is similar for a fixed distance between driving external electrodes, and the same placement within the field lines. While the field inside the conducting material is zero due to its conducting character, the Poles get charged opposite to the induced field imposed by the external driving electrodes (Fig. 3 and 7). If the potentials attained in such polarization surpass certain values specific for each reaction, a charge transfer occurs between the

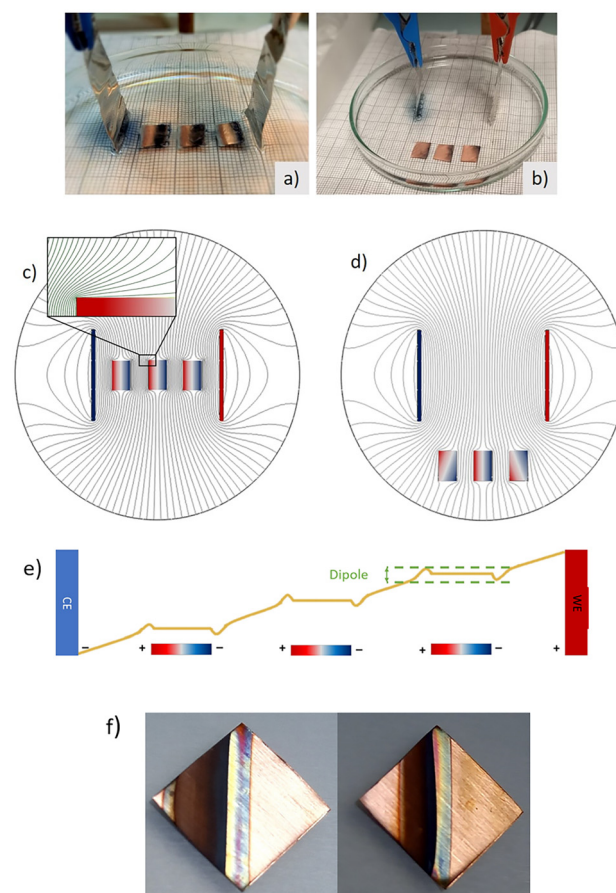


**Fig. 7** (a and b) Voltage drop unidimensional diagram across the main field direction when in presence of three metals immersed, and polarization generated at the Poles of the metal pieces. Experimental visualization of three immersed conducting copper electrodes in presence of a redox indicator based on  $[\text{SiW}_{12}\text{O}_{40}]^{-4}$  in phosphate buffer media, when applying an electric field. Positive driving electrode on the right. Induced negative pole on the left facing the external driving positive Pt electrode. A reduction of  $[\text{SiW}_{12}\text{O}_{40}]^{-4}$  anion takes place at the induced negative pole, forming a dark blue anion with 2 added electrons, while metallic copper oxidizes to  $\text{Cu}^{+2}$  at the induced anode (along with reoxidation of the  $[\text{SiW}_{12}\text{O}_{40}]^{-6}$  blue reduced at the nearby induced cathode in the second piece, allowing for a cascade of redox reactions when several bipolar Cu pieces are immersed) (c) and (d) Comsol isopotential curves in the electrolyte and immersed material, for a field created by two parallel electrodes and various positions of three immersed copper pieces. (e) Cascade effect possible in redox reactions at the electrolyte media. (f) Case in which the oxidation reaction occurs at the bipolar unwired electrode (Cu in 1 M KOH). (a–d) Reproduced from ref. 91 with permission from ECS (IOP pub), copyright 2022, and (f) reproduced from ref. 92 (RSC open access) under Creative Commons License.

electrolyte and the conducting material. Several situations are possible. Either species dissolved in the electrolyte may react, including  $\text{H}_2\text{O}$  in aqueous systems, or a reaction of the conducting material may occur, either at the negative or the positive induced Poles.

To develop this idea, it is particularly helpful to start with an example of the simplest case, a system similar to the cell culture configuration used previously (Fig. 4).<sup>88</sup> In this example no biological cells are used, but a piece of copper is





immersed in electrolyte solution containing a redox indicator  $[\text{SiW}_{12}\text{O}_{40}]^{-4}$ , which is colourless in its oxidized form and deep blue once it is reduced to  $[\text{SiW}_{12}\text{O}_{40}]^{-6}$ .<sup>91</sup> Calculations were made of the EF distortions created (Fig. 7c and d). An induced cathode was created in front of the connected driving anode, where the redox indicator gets reduced, forming a deep blue colour (Fig. 7b). Importantly, when multiple conductive pieces are immersed in the electrolyte, bipolar electrode properties are induced in each piece, depending on the alignment of the piece within the external field lines. Furthermore, if several bipolar electrodes are used a cascade effect seems to occur, since reduction products in one pole may reoxidize in the nearby positive pole, generating an additional mechanism for charge transport (Fig. 7e). The existence of reactions at the interface with the electrolyte or the material itself will depend on the reactivity in the system chosen, that is, on the potentials required for each reaction. Therefore, the arrangement of multiple arrays of conductive implanted materials can possibly amplify the external field effect.

In the described examples, if we obviate the double layer capacitive charging, a valid simplification shows that the induced  $\Delta V$  depends on the distance between the external driving electrodes, ( $d$ ), and the size of the bipolar electrode, ( $l$ ), for a specific applied voltage  $E$ , according to the equation

$$\Delta V = E \times l/d \quad (1)$$

That induced potential at the Poles is similar for all the immersed pieces of the same size, as Fig. 7a and b suggests, unless we are very close to the external driving electrodes. Since the polarization results is a deviation with respect to the lineal voltage drop (Fig. 3) in the electrolyte,  $\Delta V$  is equal in the various possible positions of the bipolar electrode, as long as it is aligned within the more intense field lines, and not too close to the driving electrodes. Fig. 7b also shows that if the pieces are removed from the zone of more intense field, the redox processes diminish and follow the same geometry of the field, with the more intense pole charging in the zones closer to the driving electrodes (Fig. 7a and b).

More complex situations exist in the case of two external parallel driving electrodes, depending on the shape of the immersed bipolar electrodes. The EF may be configured also in different geometries, using different spatial distributions of the driving electrodes, modifying their geometries and leading to different external electric fields profiles according to classical equations of electromagnetism. Thus, a pair or concentric cylindrical driving electrodes would yield a very intense field near the internal driving electrode interface and the bipolar effect will be very intense near such zone. Interdigitated driving electrodes<sup>86</sup> may also offer more complex EF geometries with rather more complex situations, while bipolar electrode functionalization may widen the electrochemical action on the biological tissue, for example, in cancer treatment and other therapies.

All examples described above suggest far reaching possibilities in which bipolar charging used in specific geometries may offer precise control of drug release (electroceuticals), rate of cell

growth or proliferation, direction of cell migration or neurite extension, and viability. There is a possibility to tailor the conditions required for specific desired cell responses by considering the bipolar effects and the known effects of such stimulation on cell physiology. They also offer a vast open field for the custom design of electric field geometries, electrode polarization, size, and geometry of immersed unwired electrodes. But even more importantly, each specific material may be tuned to the desired circumstance by considering chemical redox reactions, the possibility of ion intercalation in them, and the mixed valence gradients arising. For that reason, the study of the conducting material used as the electrode and its use as a substrate for neuron growth is essential to understand how the cell's environment changes in tandem with the material.

## Comparison of materials as bipolar electrodes in the cell culture

We proposed previously<sup>88</sup> that noble metals like Au will polarize, and that possible chemical reactions will be water oxidation or reduction at the induced anode and cathode, respectively but only at large potentials. Thus, the effects observed on Au substrates are expected to be only capacitive within the potential span of water, which was observed by the pH changes at each pole only at large potentials. On the other hand, electroactive materials that have significant conductivity and allow redox intercalation (polypyrrole, PEDOT, Iridium oxides and their hybrid derivatives) have another possible chemical reaction at much lower imposed fields than those yielding water splitting, allowing charge transfer to be limited to the immersed material.

Specifically, a possible redox reaction along the gradient of charge/potential in the induced dipole at the material would yield a gradient in oxidation state, charge carriers and the creation of ionic gradients for the ion intercalated, which is typically  $\text{Na}^+$  due to its abundance in extracellular fluids. Such charge gradients and correlated redox state gradients are expected to affect neural behaviour when a culture substratum.

Based on those hypotheses, further studies have been done on the materials using *ex situ* and *operando* conditions, with large local spatial resolution. Those include: the magnitude of the induced dipoles on the material, depending on external voltage imposed and geometry constraints, the global changes in the electrochemical cell subject to the influence of the immersed bipolar electrodes<sup>91</sup> and the ionic and oxidation state gradients in the immersed material.<sup>89–93</sup> In parallel, resistivity changes on the material surface may occur that could affect the induced dipole, and the voltage profile and ionic gradient across the bipolar immersed electrode.<sup>89,92,93</sup>

In turn, the results described below evidence that electrostimulation effects become a dynamic process, through the dynamic gradients emerging in the material. This work summarizes the effects of induced dipoles, global electrochemical cell impedance decrease in the presence of conducting materials, changes in the conducting material's redox state,



and ionic gradients. Further, it correlates those factors with the observed influence on the control of neurite growth speed and turning angle.

Our data<sup>88</sup> allowed us to establish initial material-specific correlations between unwired electrode effects, changes in physical properties, and the ionic gradients developed in the material acting as a cell substratum, but correlating those electric field effects with additional neuron behaviours remains an important area for future exploration. The data also raise new paradigmatic questions with respect to the type of material, the type of EF protocol appropriate for each required electrode geometry, and for each application (e.g., brain, spinal cord, or peripheral nerve growth). The possibility of creating coatings with specific traits will open new potential applications. For example, we used thin transparent (Fig. 4) coatings to facilitate time lapse observations, but that property might prove important for complex situations that require transparency, such as the eye (cornea or retina).

## Impedance changes in the global electrochemical cell

Impedance studies using a bipolar cell equivalent to that used for cell cultures and similar electrolytes, have shown that the immersion of conducting macroscopic pieces lowers the global electrochemical cell resistance<sup>91</sup> (Fig. 8). Even if different numbers of pieces are immersed but without physical contact, which eliminates the possibility of electronic percolation, both the electrolyte resistance and the charge transfer resistances are lowered. The effect depends on the size and geometry of the immersed conducting material and the number of pieces, but it is almost independent of the metal used, even if oxidation to soluble species occurs (e.g., for Cu<sup>92</sup>). The phenomenon is relevant to many situations, including electrochemical cell design, energy storage cells, and for applications related to tissue repair since tissue resistance changes upon wounding.<sup>112</sup>

The electrochemical cell has a significant decrease in impedance as conducting materials are immersed in the electrolyte.<sup>91</sup> Will neural cells sense a lower impedance therefore? And would that be related with inflammation parameters?

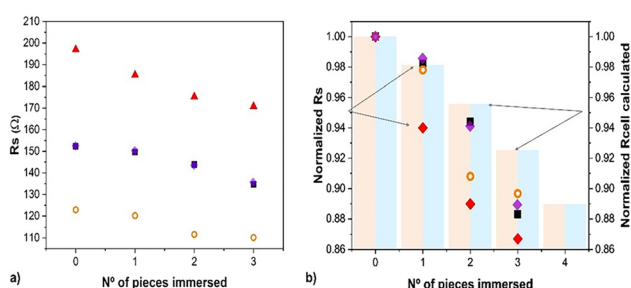


**Fig. 8** Impedance change (solution resistance,  $R_s$ , extracted from EIS fitting) depending on the number of conducting pieces immersed in various electrolytes using copper as immersed electrodes.<sup>82</sup> Blocks represent calculated COMSOL values for  $R_s$  reproduced from ref. 91 with permission from ECS (IOP pub), copyright 2022.

Significantly, recent work on the treatment of glioblastoma using gold nanoparticle electroceuticals in suspension also shows a decrease in impedance,<sup>113</sup> while carbon suspensions have also been reported to lower impedance even well beyond the percolation limit that would allow direct electric paths.<sup>114,115</sup> Therefore, the existence of conducting material in the electrolyte or cell media lowering impedance might have a direct affect in inflammatory processes that are accompanied by an impedance enhancement, raising a possible path for clinical therapies based on impedance change. Furthermore, the possible decrease in impedance also suggests a protocol for actuating through wireless electrodes in clinical protocols if lowering tissue impedance is desired.

## Conductivity changes at the material surface due to internal bipolar electrochemistry reactions

Not only does the electrolyte change its conductivity when bipolar wireless effects exist, even in absence of reactions. A relative study of the resistance across the immersed bipolar electrode has been performed after a bipolar treatment, using two contacts to discern zones at the material surface. Au bipolar electrodes show a uniform resistivity, but conductivity of PEDOT-PSS coatings decreased at both the induced anode and the induced cathode, while the center of the material remained closer in conductivity to the original coating. Despite the large error inherent in this type of measurement, the effect is reproducible and is not attributable to border effects on an untreated sample. This observation, along with reported resistivity changes *versus* oxidation states,<sup>88,115</sup> suggests that PEDOT is overoxidized at the induced anode, and reduced at the induced cathode with small changes. EDX analysis agrees because Na<sup>+</sup> intercalation due to reduction is observed at the induced cathode, while correlated colour changes are usually reported.<sup>95,116</sup> The effect is time dependent as relaxation occurs due to the existence of an ionic gradient though the material. Analogous gradients have been observed in other physical properties recently.<sup>105</sup> The case of bipolar CoN reduction yielding Co at the induced cathode is a significant example, since ferromagnetism is generated in a gradient, along with a gradient formation of Co. Time evolution of the magnetic signal is also observed after the electric field is turned off, and the material allowed to discharge<sup>105</sup> for specific configurations. This suggests future applications based on resistance or magnetization changes in biological systems as long as biocompatible materials are used.

IrOx coatings on the other hand, as predicted from reported resistances for different oxidation states,<sup>93</sup> show big changes in conductivity using this same method (Fig. 9b), with a drastic drop of conductance at the induced cathode. Therefore, the induced cathode of the material becomes almost an insulator, as the bipolar process is acting. As a consequence, the dimensions of the conducting materials are reduced and the resulting potential profile across the



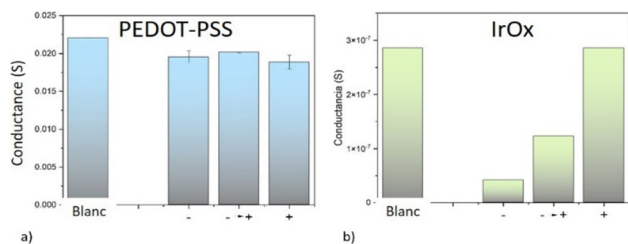


**Fig. 9** Conductance at each induced pole (– and +) and among Poles after bipolar electrochemistry in phosphate buffer for (a) PEDOT:PSS and (b) IrO<sub>x</sub>. Extracted from ref. 93 under Creative Commons License.

immersed piece suffers a drastic change, with the center being shifted towards the induced anode. As reported in the literature,<sup>90,93</sup> the changes in IrO<sub>x</sub> with redox state are much larger than in the case of PEDOT-PSS and the gradient in oxidation state involves a larger gradient in conductivity, while the induced dipole evolves with time.

Specific aspects of neurite growth could be correlated with material properties (summarised in Table 1). Significantly, neurites on the IrO<sub>x</sub> bipolar electrode grow faster,<sup>88</sup> as if they were responsive to the added dynamic variation in IrO<sub>x</sub> both in oxidation state and ionic gradient. Neurons growing on bipolar PEDOT-PSS electrodes however, show an enhanced turning angle during EF bipolar treatment, but no change in speed with respect to insulator (glass) cases. Thus, the conductivity gradient plays a role in neural growth.

In comparison, cells on a Au surface that exhibits a simple electrostatic potential gradient but without ionic or redox gradients at the material yields a significant angle of neurite turning towards the external cathode (compared to insulating glass) but no increase in speed of neurite growth. The behaviour is therefore related to the dipole induced. The neuron's response is similar to when PEDOT is used, supporting the idea that the material conductivity gradient influences specific aspects of neuron growth (direction *versus* rate of neurite advance). Cells on Pt, on the other hand, show faster neurite extension, which are similar to those for neurons on IrO<sub>x</sub>. The responses on Pt may be due to the formation of a surface platinum oxide during EF conditions.

## Redox state and ionic gradients within the conducting material

The conductivity changes and redox changes described in *ex situ* experiments have been now studied thanks to the possible local resolution of some techniques, depending on the specific material. Electron microscopy allows element identification like Na<sup>+</sup> in different bipolar electrode zones, although electron beams tend to interact and modify the redox state in these mixed conducting materials. Thus, *ex situ* experiments have been performed starting always on the reduced material side, more rich in electrons.

Studying the redox state of a material with large spatial resolution is not trivial with other techniques, like Xray diffraction. Significantly, using a synchrotron radiation source the study of the evolution in iridium oxidation states has been achieved through Xray absorption spectroscopy (XAS) has been achieved in an *operando* bipolar cell. IrO<sub>x</sub> was used as a coating on stripes of Pt coated Cycloolefin polymer.<sup>90</sup> The *operando* conditions allow to see the complex evolution due to capacitive and redox changes in the bipolar immersed material.

The photochromic properties of IrO<sub>x</sub> permit simple visual observation of changes in oxidation state across the sample, *in situ*, when a bipolar effect is created (Fig. 10). In sodium oxalate buffer (pH 3), acid medium, or in a sodium phosphate buffer (pH 7), a colour change is observed. IrO<sub>x</sub> is an intense blue colour when prepared but the induced cathode, reduced with intercalation of Na<sup>+</sup>, loses the blue color when using a 7 V per 3 cm (233 mV mm<sup>-1</sup>) external field. At larger fields (10 V per 3 cm; 333 mV mm<sup>-1</sup>), water splitting also occurs and O<sub>2</sub> and H<sub>2</sub> are observed at the induced anode and cathode, respectively. EDX evaluation of Na<sup>+</sup> intercalation *ex situ* had shown qualitatively that Na<sup>+</sup> from the buffer medium intercalates at the induced cathode of both IrO<sub>x</sub> and PEDOT materials.<sup>90,93</sup> XAS *operando* studies confirm those results (Fig. 10a and b). At a certain potential (3 or 5 V) applied externally the oxidation state of IrO<sub>x</sub> shows a reduction at the induced cathode but curiously, also at the induced anode, although to a lesser amount. When the field is stopped the reduction continues due to the capacitive charging effect. However, the unexpected propagation of reduction along the whole width of the immersed IrO<sub>x</sub> indicates that a shift of the point of zero charge is occurring. Furthermore, the material remains charged for a long time after the field has been

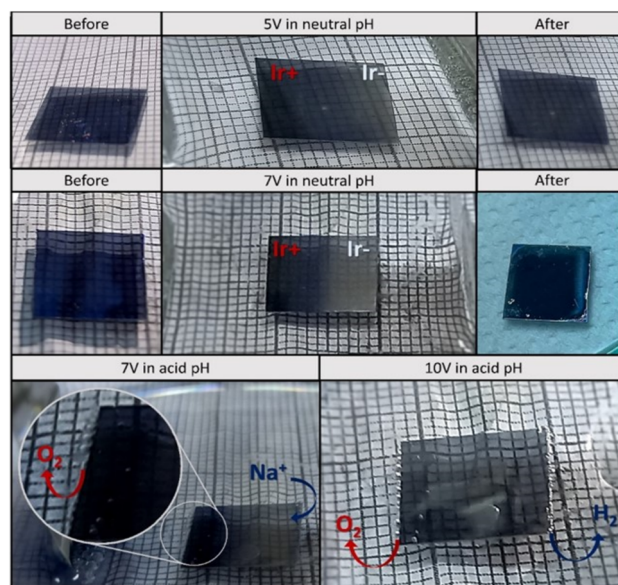


**Fig. 10** Images of the IrO<sub>x</sub> coating (on Pt coated COP) acting as bipolar electrode in a phosphate buffer and acid media electrolyte and several external potentials. Reproduced from ref. 90 with permission from ACS, copyright 2021.





switched off and the gradient in oxidation states continues to evolve for up to 2000 seconds before it eventually starts reoxidizing in air (Fig. 11a).

The kinetics of the process is faster when the external field is larger. Thus, at 7 V reduction is faster and a clear correlation exists between the time of applied voltage and oxidation state as shown by the shift in the absorption maxima for Ir LIII signal (Fig. 11b).

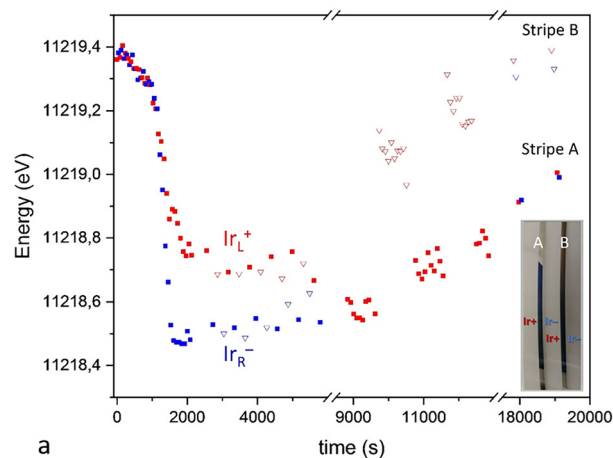
## Electrochemical global change at the electrode

The resulting IrOx material treated in bipolar conditions has a bulk electrochemical behaviour very distinct from the original one, due to the charging process, as compared with PEDOT as observed in the cyclic voltammetry (Fig. 12).<sup>93</sup> That is indeed related to a capacitive effect larger in IrOx, and a faster relaxation in PEDOT.

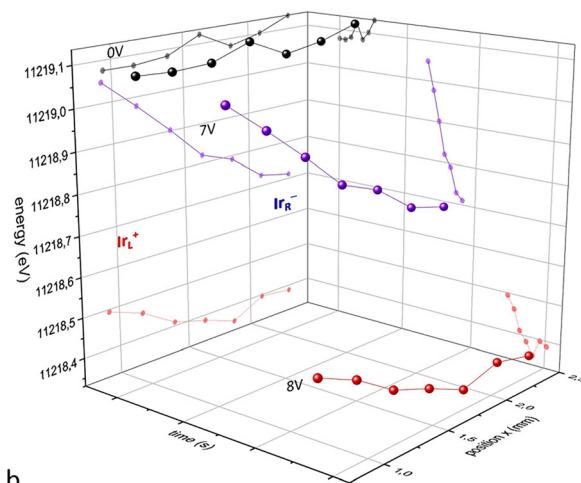
Electrostatic simulation methods reported using finite elements and shown below allow to evaluate the potential profile across the material once intercalation has occurred, and compare it with the original starting point. While PEDOT-PSS decreases in a small extent its resistance at both Poles, IrOx has a much lower conductivity at the induced cathode and therefore there is a big change in the potential induced across the material, and eventually on the Na<sup>+</sup> gradient and redox state gradients across the electrode material (Fig. 13).

The more recent studies on cobalt nitride, CoN, bipolar reduction evidence an analogous behaviour. If discharge is allowed, the process becomes reversible<sup>105</sup> and switching the device could be implemented. Simultaneously, microgradients are created that impede a full range order and crystallinity, and that are possibly tolerated better in a polymeric structure like that of PEDOT, that may change conformation with oxidation states.<sup>116</sup> Those microgradients in structure, conductivity, oxidation state, and ionic concentration, may affect the growth processes of neurons through the sensing by filopodia, which are sensitive to structures on nm scale.<sup>81</sup> A future possibility studying the nanoscale aspects of this process would be of great interest.

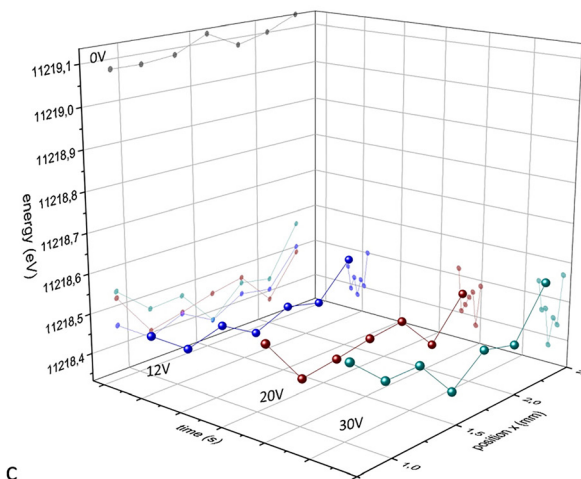
It would be expected therefore that neurons can sense a difference in relative ionic concentration. Similarly, in the case of IrOx they might perceive the persistent gradient after the treatment to permit growth cone steering, whereas the gradients in PEDOT-PSS relax faster so growth cones don't have sufficient time to respond with directional turning. The electrochemical potentials at each specific position also change, offering neurons a different chemistry depending on position, in addition to a different induced potential. Thus, a cyclic voltammetry shows an average and the dynamic of exchange between zones and therefore a wider range of redox potentials. Because *Xenopus* neurons can span many hundreds of micrometers across the material surface (extreme ends of oppositely directed neurites emerging from a single cell body) during the experiments it is possible that cells integrate multiple cues from multiple sites to yield complex responses.



a



b



c

**Fig. 11** (a) X-ray absorption energies for the Ir LIII peak during bipolar electrochemistry treatment (5 V first 10 000 seconds) and relaxation after switched off. Induced cathode shown in blue, and induced anode in red. (b) Absorption maxima for Ir LIII signal in XAS across the main axis of the bipolar immersed IrOx *in operando* conditions, for two spans of external applied voltages. The main process at IrOx occurs at 7 V imposed external voltage, while larger voltages (c) (above 10 V) involve water oxidation and reduction at the induced anode and cathode mostly. Reproduced from ref. 90 with permission from ACS, copyright 2021.



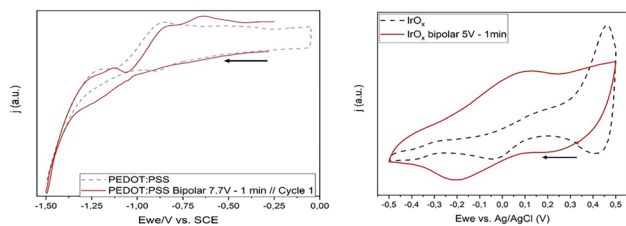


**Fig. 12** Direct contact CV experiments of bipolar electrodes after the bipolar treatment, compared with the original material prior to the bipolar effect. Extracted from ref. 93 under Creative Commons License.

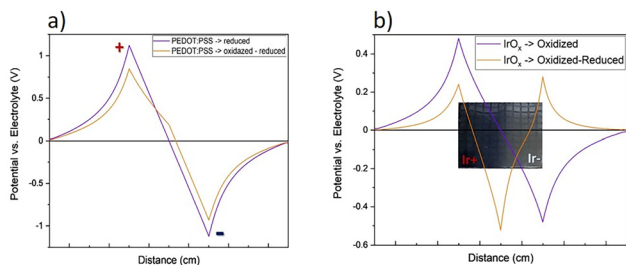


**Fig. 13** Induced potential vs. the electrolyte background at start and after the bipolar treatment for (a) PEDOT-PSS and (b) IrOx, using the observed changes in resistance for each. Extracted from ref. 93 under Creative Commons License.

## Evaluation of Induced dipoles upon external electric fields for PEDOT-PSS and IrOx bipolar electrodes

As the electrochemical processes occur at the induced cathode and anode, the resistivity of the material also changes and the voltage profile changes accordingly. Based on the gradient in resistances observed experimentally for IrOx and PEDOT-PSS coatings, the voltage distribution across the bipolar substrate material to which cells may be sensitive, may be modelled, using finite element processes. Fig. 13 shows the magnitude of the voltage gradient that the cells may feel in the material surface, apart from the electrolyte voltage drop.

For PEDOT-PSS only a small decrease of resistance was observed of the induced voltage, (Fig. 9), and consequently only small variations of the initial induced voltage across the material are determined. The magnitude of the induced voltage is in the order of  $\pm 1 \text{ V cm}^{-1}$ , in this simplified model, which corresponds to about 80 mV potential across a *Xenopus* neuron with a tip-to-tip neurite span of  $\sim 400 \mu\text{m}$ . This is a large gradient value, and possibility favors neurite turning during the application of electric field. It is relevant however to remark that at the micro and nanoscale the bipolar effect still exists in a measurable way, as described above, and the actual induced potential values are not known in such scale. However, for IrOx the reduction at the induced cathode involves a large local change in resistance, therefore involving the shift of the induced cathode towards the center of the sample, and an inversion of the initial charge at the

original cathode border of the material, (Fig. 13 voltage profile). The point of zero charge originally in the center of the sample also shifts towards the induced anode. This evolution explains the observed reduction in XAS studies above, affecting most of the sample in this configuration, and implies the creation of a negatively charged well in the material, that evolves with time. It seems logical to assume that this charge configuration prevents directionality of growth.

Thus, due to the changes in conductivity related to the material redox processes, the size of the dipole remains in PEDOT-PSS but becomes smaller in IrOx. The actual time evolution once the field is turned off is very slow, and allows for an action that persists in time.

Thus, PEDOT-PSS behaves like the case reported for Au,<sup>89</sup> although gradients in  $\text{Na}^+$  are observed in the polymer and not in Au. Confirmation of such gradients in polymers has emerged recently,<sup>117</sup> with specific designs favouring them.

Significantly the arrangement of the bipolar material electrode within the externally imposed field may modify the gradient. Thus, in the case of recent studies on CoN reduction (Fig. 14 and 15), along with magnetic changes,<sup>105</sup> a vertical bipolar electrode parallel to the external electrodes, removes the gradient across the surface, while keeping it in the direction of the field. Thus, it results in a permanent magnetic change in the vertical arrangement and a gradient that evolves with time in the horizontal arrangement.<sup>105</sup>

Whilst the simplest electric field configuration consists of parallel electrodes, other configurations of bipolar electrodes may be set, even very complex arrangements consisting of arrays, where

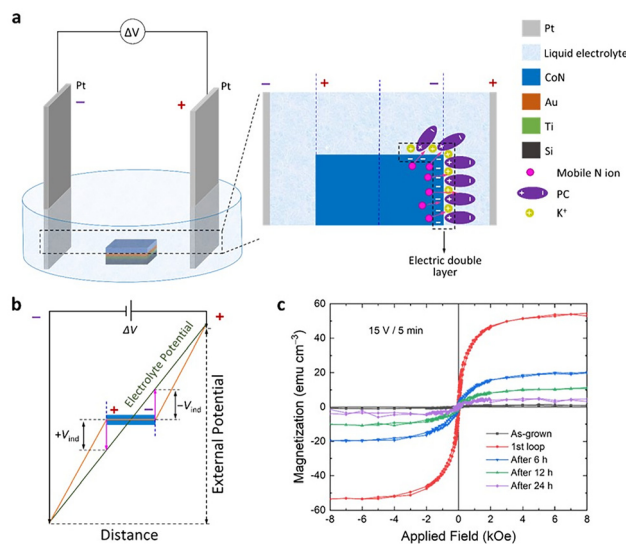


**Fig. 14** CoN coating bipolar treatment in r horizontal configuration leading to a time evolution of gradient of Co and of magnetic signal. (a) Horizontal sample orientation in the electrochemical cell and charging at the induced cathode where CoN reduction occurs and propagates. (b) Potentials induced at the bipolar electrode as described in Fig. 3. (c) Resulting magnetization and its evolution with time through relaxation of the charge gradient. Reproduced from ref. 105 under Creative Common Licence.



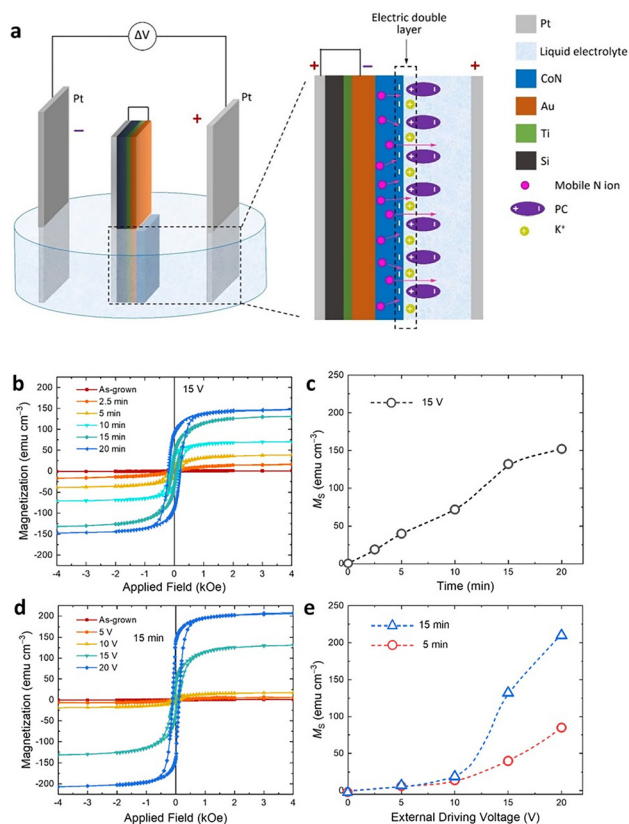


**Fig. 15** CoN bipolar treatment with induction of ferromagnetism. Vertical configuration, no gradient in CoN across the field, and permanent ferromagnetism. (a) Orientation in electric field, (b and c) magnetization depending on the time of treatment. (d and e) Magnetization achieved as a function of external driving potential applied. Reproduced from ref. 105 under Creative Commons Licence.

they can influence each other (Fig. 7), even at the nanoscale. The configuration of the driving electrodes is also important because they also define electric field geometry. For example, circular arrangements can incorporate concentric cylinders and 3d complex structures, which could be used as cuff electrodes, or to deliver spatially directed fields. Therefore, new clinical biomaterials and bioengineering research areas emerge to achieve specific gradients and electric potential profiles for each material, tuned to specific applications.

## Correlations with observed cell behaviour to date in wireless bipolar systems

Several key observations emerge from our experiments of bipolar wireless systems. Firstly, the conducting traits of either metallic or mixed valence intercalation materials have distinct behaviours in the presence of external applied fields. For example, Au does not change resistivity under bipolar conditions, rather there is only a charge polarization at the surface and only water gets oxidized or reduced at the Poles above a

certain potential (with corresponding pH change and water splitting) but not below that potential. On the other hand, PEDOT–PSS in bipolar conditions, undergoes changes in conductivity at both induced Poles, anode and cathode, though by relatively small amount, and the behaviour of neurons on it is similar to that found on Au. In both cases growth cones turn toward the external cathode (that is, the induced anode), and at much lower field intensity than on insulating substrates (e.g., glass, plastic, TiO<sub>2</sub>).

IrOx coatings undergo a larger conductivity change at the induced cathode, as expected from the reported conductivity for reduced iridium oxide. Although no turning is observed in neurite growth cones, a large increase in the speed of neurite extension is observed, indicating increased neurite extension, which would be favourable in a repair context. Based on the variation of conductivity and therefore the big change in induced potential it is not surprising that neurons sense a dynamic voltage that favours speed of growth.

The impact of Na<sup>+</sup> intercalation and Na<sup>+</sup> gradient formation may also be important since Na<sup>+</sup> content within the material is dynamic,<sup>88,92</sup> changing quickly in PEDOT–PSS after the field is turned off, but with a slow pattern in IrOx, perhaps over weeks.

Gradients in conducting polymers have also been confirmed recently.<sup>116</sup> However, relaxation of the ionic gradients is somewhat faster in the conducting polymer, at least in EDX experiments, evidencing a different situation, despite the common intercalation in both materials, IrOx and PEDOT.

Other materials subject to a bipolar treatment have shown additional gradients in redox states coupled with physical changes like ferromagnetism<sup>104</sup> which could be of use in the future for magneto therapy applications controlled through EF. That is the case of CoN coatings, where ferromagnetism disappears as the redox gradient relaxes over time in horizontal configuration. Furthermore, depending on the conductivity changes at the bipolar electrode surface, oscillating behaviour in redox states has been described<sup>91</sup> (Fig. 7f), evidencing a complex behaviour in bipolar conditions, which is material dependent.

The actual gradient in oxidation states may be considered akin to a battery potential gradient. There is a natural tendency to discharge the accumulated charge gradient, and therefore a slow discharge is observed. In the case of IrOx that fact may extend the effect of a short pulse and the stimulation during days, while in PEDOT it will be hours. Therefore, the specific protocol should be different in wireless electrostimulation scenarios, depending on the material, intercalation gradients and the changes in resistance that may accompany them. Both, DC and AC protocols are possible. Since capacitive charging may remain, an AC protocol may need to include an overpotential to induce discharge of the bipolar electrode after a previous pulse. Indeed, the field of wireless electrostimulation is still open to a wide number of studies specific for each material, each geometry of the bipolar electrode and of the global cell environment.

A summary of observed *Xenopus* neuron growth responses on different materials is presented in Table 1. It is clear that





**Table 1** Summary of main features of *Xenopus* neuron behaviour on bipolar electrodes

| Unwired bipolar conducting electrode material | EF            |                                  | Response in the material      |                     |              |                                   | Cell response            |                              |                       |                 | Material resistance (S m <sup>-1</sup> ) | Ref.         |
|---|---------------|----------------------------------|-------------------------------|---------------------|--------------|-----------------------------------|--------------------------|------------------------------|-----------------------|-----------------|--|--------------|
|   | No EF         | EF                               | Na <sup>+</sup> intercalation | Resistance gradient | Polarization | Shift in the point of zero charge | Na <sup>+</sup> gradient | Discharge of charge gradient | Faster neurite growth | Neurite turning |  |              |
|   | Cell response | Increased neuron differentiation | Na <sup>+</sup> intercalation | Resistance gradient | Polarization | Shift in the point of zero charge | Na <sup>+</sup> gradient | Discharge of charge gradient | Faster neurite growth | Neurite turning |  |              |
| Pt metal                                      | No            | No                               | No                            | No                  | Yes          | No                                | No                       | Fast                         | No                    | No              | 9 × 10 <sup>6</sup>                      | 88           |
| Au metal                                      | Yes           | No                               | No                            | No                  | Yes          | No                                | No                       | Fast                         | No                    | Yes             | 45 × 10 <sup>6</sup>                     | 88           |
| IrOx intercalating                            | No            | Yes                              | Yes                           | Yes                 | Yes          | Yes                               | Yes                      | Slow                         | Yes                   | No              | (IrO <sub>2</sub> ) ~10 <sup>6</sup>     | 88–93        |
| PEDOT–PSS intercalating                       | Yes           | Yes                              | Yes                           | Small               | Yes          | Small                             | Yes                      | Fast                         | No                    | Yes             | Range 20 to 5.4 × 10 <sup>5</sup>        | 88–93 and 95 |

IrOx differs greatly in its cell responses compared to Au and PEDOT–PSS.<sup>79</sup> In bipolar conditions cells growing on the conducting polymer develop in a similar way to those on Au in terms of differentiation (percent of cells that sprout neurites), enhancement of neurite growth (speed of neurite extension) and directionality of growth (bias of the path of the migrating growth cone). That occurs in the two cases where a maintained conductivity is observed in the material (roughly in the case of PEDOT–PSS), and even though a Na<sup>+</sup> gradient and a redox state gradient are present in PEDOT–PSS but not in Au.

Neurons on IrOx however, show different behaviours. The speed of neurite growth is faster, but no differentiation or directional turning is observed. IrOx becomes insulating at the induced cathode along the process, so the induced dipole gets spatially smaller, as well as the magnitude of the induced voltage (Fig. 3), with two positive zones across the sample (Fig. 13). Thus, the induced field observed by the neurons during growth becomes a “well” during the bipolar process and charge directionality is therefore lost. This may explain the absence of directional growth cone turning.

Therefore, the conditions where neurites grow faster correspond to the situations where there is a decrease in dipole dimensions due to a larger resistance change (IrOx). Neurite turning occurs more in cases where the dipole remains directional (PEDOT–PSS and Au) and where conductivity varies less. In the last two cases, either the Na<sup>+</sup> gradient does not exist at the material or Na<sup>+</sup> migrates faster at the material and the gradient relaxes more readily due to structural flexibility. Pt may resemble IrOx according to Table 1, and that is expected since the surface tends to form oxides.

In all cases, the impedance of the electrolyte solution decreased but less so for the IrOx case since it loses conductivity during the process and the dipole dimensions decrease, a factor that is worth exploring further.

The overarching message is that the chemistry involved in each case is determinant but the changes in physical properties are also integral to the biological response.

## Perspectives and future: the way forward

Based on the above recent observations on unwired electrodes, there are several enticing avenues opening in the near future. First, it is encouraging that the same type of materials deemed optimal as connected electrodes also show significant results as unwired bipolar electrodes. However, this field will move forward by also pursuing materials with larger complexity; hybrids of oxides and nanocarbons and/or conducting polymers since they offer a large charge capacity as described above and are crucial in emerging bipolar systems.

Available data suggest the possibility of wireless control of nerve cell growth and axon turning through the use of specific materials with conductivity/redox state changes, in the presence of an externally imposed electric fields in combination with implanted conducting materials. Prior to these findings



only connected electrodes had been used. The concept of induced ionic gradients or chemical changes due to electrochemical processes opens up ideas for novel tools to modify cell environments, including impedance modification. Moving forward electroceutical approaches based on them may include therapies for drug release through wireless methods.

Since induced currents do not need wires at the acting bipolar electrode, this opens a number of possible protocols for electrostimulation that can be incorporated into existing schemes for repair or bypass approaches that were not possible before and that eliminate the need for indwelling power packs, battery replacement, or wires (a notorious route for infection). Additional methods to induce such unwired bipolar electrodes must also be considered, as external oscillating magnetic fields may induce current in an immersed conducting material.

The use of bipolar electrochemistry also opens up the use of additional changes in physical properties at the bipolar electrode, like magnetic changes induced in a wireless way using biocompatible materials.

The possibility to use unwired electrodes with transparent coatings is exciting. The emerging field of retinal implants would clearly benefit from a means to induce specific electrical stimulation parameters using transparent conducting films, especially when patterned as an array onto a flexible biocompatible flexible substrate. IrOx and conducting polymers (Fig. 2) permit use in such situations where transparency is essential. The cornea is highly innervated and corneal wound healing is facilitated by a functional nerve supply, so a transparent bipolar electrode 'contact lens' may prove useful for corneal graft procedures or after corneal injury.

Those possibilities will be greatly dependent on an optimal design of the geometry of the induced electric field on the implanted material, and the geometry of the material itself, its functionalization, transparency, and biocompatibility. A key point is represented by the distance between external electrodes, which will necessarily be far from the target tissue *in vivo*. Thus, electrodes placed further apart would need larger potentials applied to induce a specific potential at the immersed unwired electrode if a parallel configuration is used. But a cylindrical concentric geometry would induce a larger potential near the inner driving electrode, overcoming such serious drawback, and this would be particularly apt for nerve tissues. More complex geometries like interdigitated electrodes may also soften the driving applied potentials.

The new materials developed and reported here are evidence that further studies would benefit from the combinations of conducting carbon components with intercalation mixed valence materials, like those found in IrOx–nanocarbon hybrids or conducting polymers with nanostructure. Using these in wireless configurations is enticing because carbon, even as hybrids with IrOx, will enhance conductivity during the process. New prospective materials include those where magnetic changes occur during the electric field action, such as organic radicals or iron oxide nanoparticles, and also the widely used titanium based implants with nanopatterned structures given their large biocompatibility.<sup>118</sup>

It is worthwhile to include varying EF protocols in the future to may induce DC and AC polarization switching between Poles at frequencies similar or dissimilar from that of the neural system, modifying action (functional bypass) as well as repair, depending on the specific time and voltage parameters. Thus, lowering the impedance of the medium would affect inflammatory processes, and immunological factors, enhancing the prospect for tissue healing.

Looking from the cell's point of view it will be crucial to understand how different cell types react to diverse stimulation protocols, configurations, and materials. Given the importance of ion gradients in bipolar stimulation further insight is required to determine how such gradients are read and interpreted by cells. Here we emphasized the role of Na<sup>+</sup> but would gradients of other physiologically important ions, such as Ca<sup>+2</sup> or K<sup>+</sup> induce similar responses?

Studies of the effects on the interaction with alternative biological cells and models are desirable, but also more detail regarding the polarization occurring on electroactive nanoparticles which are not fixed in space (that is, free floating in the cell, medium, or extracellular fluids). Thus, a significant theoretical study of the physical parameters behind wireless bipolar electrochemistry is envisaged as necessary when nanoparticles are used as electroceuticals or as impedance changers.

Above all, if electrostimulation is possible with unwired bipolar electrodes, is there a way to induce such polarization without driving electrodes? The reported magnetic oscillation described inducing current on a self-rectifier system suggests so. This additional step in the creation of an unwired electrode would open significantly access to electrostimulation on implanted small conductive pieces, or even nanoparticles. The field of application would then get reflected in neural repair, and other therapeutic objectives related to drug release (in cancer *etc.*), electroporation *etc.*

Within the growing sphere of possibilities one is outstanding. Are neurons themselves able to induce polarization of the implanted conducting material, and therefore be affected also by it? Some experiments described above suggest that is the case. Therefore, all conducting materials studied previously should be reconsidered during cell culture or *in vivo* tests, including their changes in oxidation states and conductivity. This would need to be done for each specific case based on size, topography, 2D or 3D structure, geometry and field arrangement, and if possible with knowledge of the inner redox gradient.

Thus, we may imagine *in vivo* stimulation of retina by immersion of conducting nanoparticles or planar transparent coatings as those described here, with a bipolar field induced through external electrodes far from the retina. On a spinal cord implant, the driving electrodes could be far from the actual wound, not interfering with the growth. Nanopatterning of the conducting material is also possible to crate paths for growing cells. Although complex, the data and practical clinical applications could prove electrifying.

In conclusion, the recent demonstration that bipolar stimulation is possible in conductive materials and that it influences



neuron growth opens a wide new field for innovative electrostimulation prospects. Future action requires significant *in situ* study of materials and the global arrangement of bipolar or multipolar electrodes *in vitro* and *in vivo*. There are implications for diverse therapies affecting the nervous system, skin, retina implants, cardiac stimulation, and many more yet to emerge.

## Author contributions

This perspective article has been built through the interactive work of two researchers in two fields highly complementary in terms of bio studies and materials for electrodes as well as electrochemistry. It has focussed specifically on the new aspects found on cell behaviour due to the induction of wireless effects.

## Conflicts of interest

There are no conflicts to declare.

## Acknowledgements

The authors want to thank financial contribution from Grants from Fundacion MARATO TV3 2011 (110131), Spain AEI (ref MAT2015-65192-R, RTI2018-097753-B-I00, PID2021-123276OB-I00, CEX2019-000917-S).

## References

- 1 B. R. Stewart, L. Erskine and C. D. McCaig, Calcium Channel Subtypes and Intracellular Calcium Stores Modulate Electric Field-Stimulated and Oriented Nerve Growth, *Dev. Biol.*, 1995, **171**, 340–351.
- 2 C. D. McCaig, A. M. Rajniecek, B. Song and M. Zhao, Has electrical growth cone guidance found its potential?, *Trends Neurosci.*, 2002, **25**, 354–359.
- 3 C. D. McCaig, A. M. Rajniecek, B. Song and M. Zhao, Controlling cell behaviour electrically: current views and future potential, *Physiol. Rev.*, 2005, **85**, 943–978.
- 4 A. M. Rajniecek, Electric field effects on neuronal growth cone guidance, in *The Physiology of Bioelectricity in Development, Tissue Regeneration and Cancer: Weak Electric Field Effects on Cells, Sub-cellular Systems and Tissues*, ed. C. E. Pullar, CRC Press, Taylor and Francis Group LLC, Boca Raton, FL, 2011, pp. 201–232.
- 5 C. D. McCaig, B. Song and D. A. M. Rajniecek, Electrical dimensions in cell science, *J. Cell Sci.*, 2009, **122**, 4267–4276, DOI: [10.1242/jcs.023564](https://doi.org/10.1242/jcs.023564).
- 6 L. Matter, B. Harland, B. Raos, D. Svirskis and M. Asplund, Generation of direct current electrical fields as regenerative therapy for spinal cord injury: A review, *APL Bioeng.*, 2023, **7**, 031505.
- 7 S. Asirvatham, K. Londoner, M. Aravamudan, T. Deering, H. Heidebuchel, S. Kapa, B. Keenan, E. Maor, S. Mattke, L. T. Middleton, V. Pavlov and D. Weber, Building a bioelectronic medicine movement 2019: insights from leaders in industry, academia, and research., *Bioelectronic Medicine*, 2020, **6**, 1.
- 8 C. C. McIntyre and W. M. Grill, Excitation of Central Nervous System Neurons by Nonuniform Electric Fields, *Biophys. J.*, 1999, **76**, 878–888.
- 9 S. F. Cogan, Neural Stimulation and Recording Electrodes, *Annu. Rev. Biomed. Eng.*, 2008, **10**, 275–309.
- 10 D. R. Merrill, M. Bikson and J. G. R. Jefferys, Electrical stimulation of excitable tissue: design of efficacious and safe protocols, *J. Neurosci. Methods*, 2005, **141**, 171–198.
- 11 X. S. Zheng, C. Tan, E. Castagnola and X. T. Cui, Electrode Materials for Chronic Electrical Microstimulation, *Adv. Healthc. Mater.*, 2021, **10**, e2100119, DOI: [10.1002/adhm.202100119](https://doi.org/10.1002/adhm.202100119).
- 12 P. C. Harikesh, C.-Y. Yang, D. Tu, J. Y. Gerasimov, A. M. Dar, A. Armada-Moreira, M. Massetti, R. Kroon, D. Bliman, R. Olsson, E. Stavrinidou, M. Berggren and S. Fabiano, Organic electrochemical neurons and synapses with ion mediated spiking, *Nat. Commun.*, 2022, **13**, 901, DOI: [10.1038/s41467-022-28483-6](https://doi.org/10.1038/s41467-022-28483-6).
- 13 P. Heiduschka and S. Thanos, Implantable Bioelectronic Interfaces for lost nerve functions, *Prog. Neurobiol.*, 1988, **55**, 433–461.
- 14 W. Cho, S.-H. Yoon and T. D. Chung, Streamlining the interface between electronics and neural systems for bidirectional electrochemical communication, *Chem. Sci.*, 2023, **14**, 4463.
- 15 R. Feiner and T. Dvir, Tissue–electronics interfaces: from implantable devices to engineered tissues, *Nat. Rev. Mater.*, 2018, **3**, 17076.
- 16 H. Lorach, A. Galvez, V. Spagnolo, F. Martel, S. Karakas, N. Interling, M. Vat, O. Faivre, C. Harte, S. Komi, J. Ravier, T. Collin, L. Coquoz, I. Sakr, E. Baaklini, S. D. Hernandez-Charpak, G. Dumont, R. Buschman, N. Buse, T. Denison, I. van Nes, L. Asboth, A. Watrin, L. Struber, F. Sauter-Starace, L. Langar, V. Auboiroux, S. Carda, S. Chabardes, T. Aksenova, R. Demesmaeker, G. Charvet, J. Bloch and G. Courtine, Walking naturally after spinal cord injury using a brain–spine interface, *Nature*, 2023, **618**, 126–133.
- 17 M. A. Rahman, S. Walia, S. Naznee, M. Taha, S. Nirantar, F. Rahman, M. Bhaskaran and S. Sriram, Artificial somatosensors: feedback receptors for electronic skins, *Adv. Intell. Syst.*, 2020, **2**, 2000094.
- 18 M. Bacova, K. Bimbova, A. Kisucka, N. Lukacova and J. Galik, Epidural oscillating field stimulation increases axonal regenerative capacity and myelination after spinal cord trauma, *Neural Regener. Res.*, 2022, **17**, 2730–2736.
- 19 J. Cervera, M. Levin and S. Mafe, Bioelectricity of non-excitable cells and multicellular pattern memories: Biophysical modeling, *Phys. Rep.*, 2023, **1004**, 1–31.





- 20 T. K. Leslie and W. J. Brackenbury, Sodium channels and the ionic microenvironment of breast tumours, *J. Physiol.*, 2023, **601**, 1543–1553.
- 21 M. R. Silic and G. Zhang, Bioelectricity in Developmental patterning and size control: evidence and genetically encoded tools in the zebrafish model, *Cells*, 2023, **12**, 1148.
- 22 E. Lagasse and M. Levin, Future medicine: from molecular pathways to the collective intelligence of the body, *Trends Mol. Med.*, 2023, **29**, 687–710.
- 23 A. M. Rajnicek, R. Stump and K. R. Robinson, An endogenous sodium current may mediate wound healing in *Xenopus* neurulae, *Dev. Biol.*, 1998, **128**, 290–299.
- 24 A. T. Barker, L. F. Jaffe and J. W. Vanable Jr., The glabrous epidermis of cavies contains a powerful battery, *Am. J. Physiol.: Regul., Integr. Comp. Physiol.*, 1982, **242**, R358–R366.
- 25 B. Song, M. Zhao, J. V. Forrester and C. D. McCaig, Nerves are guided and nerve sprouting is stimulated by a naturally occurring electrical field in vivo, *J. Cell Sci.*, 2004, **117**, 4681–4690.
- 26 D. Vanel, V. Barth, R. Davies, I. S. Fentimen, R. Holland, J. L. Lamarque, V. Sacchini and I. Schreer, Electropotential evaluation as a new technique for diagnosing breast lesions, *Eur. J. Radiol.*, 1997, **24**, 33–3827.
- 27 M. Szatkowski, M. Mycielska, A.-L. Kho and M. B. A. Djamgoz, Electrophysiological recordings from the rat prostate gland in vitro: Identified single-cell and transepithelial (lumen) potentials, *BJU Int.*, 2000, **86**, 1068–1075.
- 28 A. Polak, L. C. Kloth, E. Blaszcak, J. Taradaj, A. Nawrat-Szoltysik, A. Walczak, L. Bialek, M. Paczula, A. Franek and C. Kucio, Evaluation of the Healing Progress of Pressure Ulcers Treated with Cathodal High-Voltage Monophasic Pulsed Current: Results of a Prospective, Double-blind, Randomized Clinical Trial, *Adv. Skin Wound Care*, 2016, **29**(10), 447–459.
- 29 B. Baniya, M. Tebyani, N. Aseffeyzabadi, T. Nguyen, C. Hernandez, K. Zhu, H. Li, J. Selberg, H. Hsieh, P. Pansodtee, H. Yang, C. Recendez, G. Keller, W. S. Hee, E. Aslankoochi, R. R. Isserof, M. Zhao, M. Gomez, M. Rolandi and M. Teodorescu, A system for bioelectronic delivery of treatment directed toward wound healing, *Sci. Rep.*, 2023, **13**, 14766.
- 30 J. W. Vanable Jr., L. L. Hearson and M. E. McGinnis, The role of endogenous electrical fields in limb regeneration, *Prog. Clin. Biol. Res.*, 1983, **110**(PtA), 587–596.
- 31 D. S. Adams, A. Masi and M. Levin,  $H^+$  pump-dependent changes in membrane voltage are an early mechanism necessary and sufficient to induce tail regeneration, *Development*, 2007, **134**, 1325–1335.
- 32 B. Reid, B. Song and M. Zhao, Electric currents in *Xenopus* tadpole tail regeneration, *Dev. Biol.*, 2009, **335**, 198–207.
- 33 C. M. Illingworth and A. T. Barker, Measurement of electrical currents emerging during the regeneration of amputated fingertips in children, *Clin. Phys. Physiol. Meas.*, 1980, **1**, 87–89.
- 34 K. Hotary and K. R. Robinson, The neural tube of the *Xenopus* embryo maintains a potential difference across itself, *Dev. Brain Res.*, 1991, **59**, 65–73.
- 35 R. B. Borgens and R. Shi, Uncoupling histogenesis from morphogenesis in the vertebrate embryo by collapse of the transneural tube potential, *Dev. Dyn.*, 1995, **203**, 456–467.
- 36 H. C. Leung, C. Leclerc, M. Moreau, A. M. Shipley, A. L. Miller and S. E. Webb, Transmembrane  $H^+$  fluxes and the regulation of neural induction in *Xenopus laevis*, *Zygote*, 2022, **30**, 267–278.
- 37 R. B. Borgens, L. F. Jaffe and M. J. Cohen, Large and persistent electrical currents enter the transected lamprey spinal cord, *Proc. Natl. Acad. Sci. U. S. A.*, 1980, **77**, 1209–1213.
- 38 M. Zuberi, P. Liu-Snyder, A. ul Haque, D. M. Porterfield and R. B. Borgens, Large naturally-produced electric currents and voltage traverse damaged mammalian spinal cord, *J. Biol. Eng.*, 2008, **2**, 17.
- 39 A. M. Rajnicek, L. E. Foubister and C. McCaig, Temporally and spatially coordinated roles for Rho, Rac, Cdc42 and their effectors in growth cone guidance by a physiological electric field, *J. Cell Sci.*, 2006, **119**, 1723–1735.
- 40 A. M. Rajnicek, L. E. Foubister and C. McCaig, Growth cone steering by a physiological electric field requires dynamic microtubules, microfilaments and Rac-mediated filopodial asymmetry, *J. Cell Sci.*, 2006, **119**, 1736–1745.
- 41 J. I. Hoare, A. M. Rajnicek, C. D. McCaig, R. N. Barker and H. M. Wilson, (2016). Electric fields are novel determinants of human macrophage functions, *J. Leukocyte Biol.*, 2016, **99**, 1141–1151.
- 42 C. E. Arnold, A. M. Rajnicek, J. L. Hoare, S. M. Pokharel, C. D. McCaig, R. N. Barker and H. Wilson, Physiological strength electric fields modulate human T-cell activation and polarisation, *Sci. Rep.*, 2019, **9**, 17604.
- 43 T. J. Schwedt and B. Vargas, Neurostimulation for Treatment of Migraine and Cluster Headache, *Pain Med.*, 2015, **16**, 1827–1834.
- 44 J. Huang, S. Xue, P. Buchmann, A. P. Teixeira and M. Fussenegger, An electrogenetic interface to program mammalian gene expression by direct current, *Nat. Metab.*, 2023, **5**, 1395–1407.
- 45 S. Harkema, Y. Gerasimenko, J. Hodes, J. Burdick, C. Angeli, Y. Chen, C. Ferreira, A. Willhite, E. Rejc, R. G. Grossman and V. R. Edgerton, Effect of epidural stimulation of the lumbosacral spinal cord on voluntary movement, standing, and assisted stepping after motor complete paraplegia: a case study, *Lancet*, 2011, **377**, 1938–1947.
- 46 R. Van den brand, J. Heutschi, Q. Barraud, J. Digiovanna, K. Bartholdi, M. Huerlimann, L. Friedli, I. Vollenweider, E. M. Moraud, S. Duis, N. Dominici, S. Micera, P. Musienko and G. Courtine, Restoring Voluntary Control of Locomotion after Paralyzing Spinal Cord Injury, *Science*, 2012, **336**, 1182–1185.



- 47 S. Chandrasekaran, N. A. Bhagat, R. Ramdeo, S. Ebrahimi, P. D. Sharma, D. G. Griffin, A. Stein, S. J. Harkema and C. E. Bouton, Targeted transcutaneous spinal cord stimulation promotes persistent recovery of upper limb strength and tactile sensation in spinal cord injury: a pilot study, *Front. Neurosci.*, 2023, **17**, 1210328.
- 48 L. J. Moriarty and R. B. Borgens, An oscillating extracellular voltage gradient reduces the density and influences the orientation of astrocytes in injured mammalian spinal cord, *J. Neurocytol.*, 2001, **30**, 45–57.
- 49 N. Mekhail, R. M. Levy, T. R. Deer, L. Kapural, S. Li, K. Amirdelfan, C. W. Hunter, S. M. Rosen, S. J. Costandi, S. M. Falowski, A. H. Burgher, J. E. Pope, C. A. Gilmore, F. A. Qureshi, P. S. Staats, J. Scowcroft, J. Carlson, C. K. Kim, M. I. Yang, T. Stauss and L. Pore, Long-term safety and efficacy of closed-loop spinal cord stimulation to treat chronic back and leg pain (Evoke): a double-blind, randomised, controlled trial, *Lancet Neurol.*, 2019, **19**, 123–134.
- 50 D. Yarnitsky, D. W. Dodick, B. M. Grosberg, R. Burstein, A. Ironi, D. Harris, T. Lin and S. D. Silberstein, Remote Electrical Neuromodulation (REN) Relieves Acute Migraine: A Randomized, Double-Blind, Placebo-Controlled, Multicenter Trial, *Headache*, 2019, **59**, 1240–1252.
- 51 R. R. Vikram, K. K. Sellers, D. L. Wallace, M. M. Shanechi, H. E. Dawes and E. F. Chang, Direct Electrical Stimulation of Lateral Orbitofrontal Cortex Acutely Improves Mood in Individuals with Symptoms of Depression, *Curr. Biol.*, 2018, **28**, 3893–3902.
- 52 M. J. McKasson, L. Huang and K. R. Robinson, Embryonic Schwann cells migrate anodally in small electric fields, *Exp. Neurol.*, 2008, **211**, 585–587.
- 53 C. T. Tsui, P. Lal, K. V. R. Fox, M. A. Churchward and K. G. Todd, The effects of electrical stimulation on glial cell behavior, *BMC Biomed. Eng.*, 2022, **4**, 7.
- 54 J. W. Salatino, K. A. Ludwig, T. D. Y. Kozai and E. K. Purcell, Glial responses to implanted electrodes in the brain, *Nat. Biomed. Eng.*, 2017, **862**, 862–877.
- 55 J. S. Jara, S. Agger and E. R. Hollis, Functional electrical stimulation and the modulation of the axon regeneration program, *Front. Cell Dev. Biol.*, 2020, **8**, 736.
- 56 R. B. Borgens, A. R. Blight and M. E. McGinnis, Behavioral recovery induced by applied electric fields after spinal cord hemisection in guinea pig, *Science*, 1987, **238**, 366–369.
- 57 R. B. Borgens, A. R. Blight and M. E. McGinnis, Functional recovery after spinal cord hemisection in guinea pigs: the effects of applied electric fields, *J. Comp. Neurol.*, 1990, **296**, 634–653.
- 58 R. B. Borgens, J. P. Toombs, A. R. Blight, M. E. McGinnis, M. S. Bauer, W. Widmer and J. R. Cook Jr., Effects of applied electrical fields on clinical cases of complete paraplegia in dogs, *Restor. Neurol. Neurosci.*, 1993, **5**, 305–322.
- 59 R. B. Borgens, J. P. Toombs, G. Breur, W. R. Widmer, D. Water, A. M. Harbath, P. March and L. G. Adams, An imposed oscillating electrical field improves the recovery of function in neurologically complete paraplegic dogs, *J. Neurotrauma*, 1999, **16**, 639–657.
- 60 S. Shapiro, R. Borgens, R. Pascuzzi, K. Roos, M. Groff, S. Purvines, R. B. Rodgers, S. Hagy and P. Nelson, Oscillating field stimulation for complete spinal cord injury in humans: a Phase 1 trial, *J. Neurosurg. Spine*, 2005, **2**, 3–10.
- 61 M. P. Lichtenstein, E. Pérez, L. Ballesteros, C. Suñol and N. Casañ-Pastor, Short term electrostimulation enhancing neural repair in vitro using large charge capacity intercalation electrodes, *Appl. Mater. Today*, 2017, **6**, 29–43.
- 62 T. Milekovic, E. M. Moraud, N. Macellari, *et al.*, A spinal cord neuroprosthesis for locomotor deficits due to Parkinson's disease, *Nat. Med.*, 2023, **29**, 2854–2865.
- 63 J. G. Troughton, Y. O. Ansong Snr, N. Duobaite and C. M. Proctor, Finite element analysis of electric field distribution during direct current stimulation of the spinal cord: implications for device design, *APL Bioeng.*, 2023, **7**, 046109.
- 64 R. Ramasubbu, S. Lang and Z. H. T. Kiss, Dosing of Electrical Parameters in Deep Brain Stimulation (DBS) for Intractable Depression: A Review of Clinical Studies, *Front. Psychiatry*, 2018, **9**, 302.
- 65 N. Casañ-Pastor, Nanocarbon-Iridium Oxide Nanostructured Hybrids as Large Charge Capacity Electrostimulation Electrodes for Neural Repair, *Molecules*, 2021, **26**, 4236.
- 66 A. M. Rajnicek, C. Suñol and N. Casan-Pastor, Nanostructured Electroactive Materials with Large Charge Capacity: Direct Field Electrostimulation through Connected and Non-connected Electrodes, in *Engineering Biomaterials for Neural Applications. Targeting traumatic Brain and spinal cord Injuries*, ed. E. Lopez-Dolado and M. C. Serrano, Springer Nature, ch. 5, 2022, pp. 99–125.
- 67 R. Green and M. R. Abidian, Conducting Polymers for Neural Prosthetic and Neural Interface Applications, *Adv. Mater.*, 2015, **27**, 7620–7637.
- 68 N. M. Carretero, M. P. Lichtenstein, E. Pérez, L. Cabana, C. Suñol and N. Casañ-Pastor, IrOx-Carbon Nanotubes Hybrid: A Nanostructured Material for Electrodes with Increased Charge Capacity in Neural systems, *Acta Biomater.*, 2014, **10**, 4548–4558.
- 69 N. M. Carretero, M. P. Lichtenstein, E. Pérez, S. Sandoval, G. Tobias, C. Suñol and N. Casan-Pastor, Enhanced Charge Capacity in Iridium Oxide-Graphene Oxide Hybrids, *Electrochim. Acta*, 2015, **157**, 369–377.
- 70 E. Pérez, M. P. Lichtenstein, C. Suñol and N. Casan-Pastor, Coatings of Nanostructured Pristine Graphene-IrOx Hybrids for Neural Electrodes: Layered Stacking and the role of non-oxygenated Graphene, *Mater. Sci. Eng., C*, 2015, **55**, 218–226.
- 71 M. P. Lichtenstein, N. M. Carretero, E. Pérez, M. Pulido-Salgado, J. Moral-Vico, C. Solà, N. Casañ-Pastor and C. Suñol, Biosafety assessment of conducting nanostructured materials by using co-cultures of neurons and astrocytes, *Neurotoxicology*, 2018, **68**, 115–125.



- 72 R. Balint, N. J. Cassidy and S. H. Cartmell, S. H. (2014). Conductive polymers: Towards a smart biomaterial for tissue engineering, *Acta Biomater.*, 2014, **10**, 2341–2353.
- 73 N. P. Pampaloni, M. Lottner, M. Giugliano, A. Matruglio, F. D'Amico, M. Prato, J. A. Garrido, L. Ballerini and D. Scaini, Single-layer graphene modulates neuronal communication and augments membrane ion currents, *Nat. Nanotechnol.*, 2018, **13**, 755–764.
- 74 K. Kostarelos, M. Vincent, C. Hebert and J. A. Garrido, Graphene in the Design and Engineering of Next-Generation Neural Interfaces, *Adv. Mater.*, 2017, **29**, 1700909.
- 75 K. Wissel, G. Brandes, N. Pütz, G. L. Angrisani, J. Thieleke, T. Lenarz and M. Durisin, Platinum corrosion products from electrode contacts of human cochlear implants induce cell death in cell culture models, *PLoS One*, 2018, **13**, e0196649.
- 76 S. Negi, R. Bhandari, L. Rieth and F. Solzbacher, *In vitro* comparison of sputtered iridium oxide and platinum-coated neural implantable microelectrode arrays, *Biomed. Mater.*, 2010, **5**, 015007.
- 77 A. M. Cruz, L. L. Abad, N. M. Carretero, J. Moral-Vico, J. Fraxedas, P. Lozano, G. Subías, V. Padial, M. Carballo, J. E. Collazos-Castro and N. Casañ-Pastor, Iridium Oxohydroxide, a Significant Member in the Family of Iridium Oxides. Stoichiometry, Characterization, and Implications in Bioelectrodes, *J. Phys. Chem. C*, 2012, **116**, 5155–5168.
- 78 J. Moral-Vico, N. M. Carretero, E. Perez, C. Suñol, M. Lichtenstein and N. Casañ-Pastor, Dynamic electrodeposition of aminoacid-polypyrrole on aminoacid-PEDOT substrates: Conducting polymer bilayers as electrodes in neural systems, *Electrochim. Acta*, 2013, **111**, 250–260.
- 79 A. F. Girão, J. Sousa, A. Domínguez-Bajo, A. González-Mayorga, I. Bdikin, E. Pujades-Otero, N. Casañ-Pastor, M. J. Hortigüela, G. Otero-Irurueta, A. Completo, M. C. Serrano and P. A. A. P. Marques, 3D reduced graphene oxide scaffolds with a combinatorial fibrous-porous architecture for neural tissue engineering, *ACS Appl. Mater. Interfaces*, 2020, **12**, 38962–38975.
- 80 K. Baranes, N. Chejanovsky, N. Alon, A. Sharoni and O. Shefi, Topographic cues of nano-scale height direct neuronal growth pattern, *Biotechnol. Bioeng.*, 2012, **109**, 1791–1797.
- 81 A. M. Rajnicek, S. Britland and C. McCaig, Contact guidance of CNS neurites on grooved quartz: influence of groove dimensions, neuronal age and cell type, *J. Cell Sci.*, 1997, **110**, 2905–2913.
- 82 M. Bianchi, S. Guzzo, A. Lunghi, P. Greco, A. Pisciotta, M. Murgia, G. Carnevale, L. Fadiga and F. Biscarini, Synergy of Nanotopography and Electrical Conductivity of PEDOT/PSS for Enhanced Neuronal Development, *ACS Appl. Mater. Interfaces*, 2023, **15**, 59224–59235.
- 83 N. Royo-Gascon, M. Wininger, J. I. Scheinbeim, B. L. Firentein and W. Craelius, Piezoelectric Substrates Promote Neurite Growth in Rat Spinal Cord Neurons, *Ann. Biomed. Eng.*, 2013, **41**, 112–122.
- 84 A. Ehrlicher, T. Betz, B. Stuhmann, D. Koch, V. Milner, M. G. Raizen and J. Kas, Guiding neuronal growth with light, *Proc. Natl. Acad. Sci. U. S. A.*, 2002, **9**, 16024–16028.
- 85 H. Kim, S. Park, G. Housler, V. Marcel, S. Cross and M. Izadjoo, An overview of the efficacy of a next generation electroceutical wound care device, *Mil. Med.*, 2016, **181**, 184–190.
- 86 R. J. Forster, Wirefree electroceuticals: 3D electrical and electrochemical stimulation of biological systems, *Curr. Opin. Electrochem.*, 2023, **39**, 101297.
- 87 J. C. Chen, G. Bhave, F. Alrashdan, A. Dhuliyawalla, K. J. Hogan, A. G. Mikos and J. T. Robinson, Self-rectifying magnetoelectric metamaterials for remote neural stimulation and motor function restoration, *Nat. Mater.*, 2023, **23**, 139–146.
- 88 A. M. Rajnicek, Z. Zhao, J. Moral-Vico, A. M. Cruz, C. D. McCaig and N. Casañ-Pastor, Controlling Nerve Growth with an Electric Field Induced Indirectly in Transparent Conductive Substrate Materials, *Adv. Healthcare Mater.*, 2018, **7**, 1800473.
- 89 L. L. Abad, A. Rajnicek and N. Casañ-Pastor, Electric Field Gradients and Bipolar Electrochemistry effects on Neural Growth. A finite element study on immersed electroactive conducting electrode materials, *Electrochim. Acta*, 2019, **317**, 102–111.
- 90 L. Fuentes-Rodríguez, L. Abad, L. Simonelli, D. Tonti and N. Casañ-Pastor, Iridium oxide redox gradient material: Operando X Ray absorption of Ir gradient oxidation states during IrOx bipolar electrochemistry, *J. Phys. Chem. C*, 2021, **125**, 16629–16642.
- 91 L. Fuentes-Rodríguez, L. L. Abad, E. Pujades, P. Gómez-Romero, D. Tonti and N. Casañ-Pastor, Dramatic drop in cell resistance through induced dipoles and bipolar electrochemistry, *J. Electrochem. Soc.*, 2022, **169**, 016508.
- 92 L. Fuentes-Rodríguez, E. Pujades, J. Fraxedas, A. Crespi, K. Xu, L. Abad and N. Casañ-Pastor, Oscillatory Patterns in Redox Gradient Materials through Wireless Bipolar Electrochemistry. The dynamic wave-like case of copper bipolar oxidation, *Mater. Chem. Front.*, 2022, **6**, 2284–2296.
- 93 L. Fuentes-Rodríguez, Ph. D thesis defense., Universitat Autònoma de Barcelona, *Electroquímica inalàmbrica bipolar: Nuevos hitos y aplicaciones*, 2022, Last Access, jan 2024 <https://www.tdx.cat/handle/10803/688078?locale-attribute=es>.
- 94 M. Fleischmann, J. Ghoroghchian, D. Rolison and S. Pons, Electrochemical Behavior of Dispersions of Spherical Ultramicroelectrodes, *J. Phys. Chem.*, 1986, **90**, 6392.
- 95 S. O. Krabbenborg and J. Huskens, Electrochemically generated gradients, *Angew. Chem., Int. Ed.*, 2014, **53**, 9152–9167.
- 96 G. Loget, D. Zigah, L. Bouffier, N. Sojic and A. Kuhn, Bipolar Electrochemistry: From Materials Science to Motion and Beyond, *Acc. Chem. Res.*, 2013, **46**, 2513–2523.





- 97 N. Shida, Y. Zhou and S. Inagi, Bipolar Electrochemistry: A Powerful Tool for Electrifying Functional Material Synthesis, *Acc. Chem. Res.*, 2019, **52**, 2598–2608.
- 98 L. Koefoed, S. U. Pedersen and K. Daasbjerg, Bipolar electrochemistry— A wireless approach for electrode reactions, *Curr. Opin. Electrochem.*, 2017, **2**, 13–17.
- 99 G. Tisserant, Z. Fattah, C. Ayela, J. Roche, B. Plano, D. Zigah, B. Goudeau, A. Kuhn and L. Bouffier, Generation of metal composition gradients by means of bipolar electrodeposition, *Electrochim. Acta*, 2015, **179**, 276–281.
- 100 S. Inagi, Fabrication of gradient polymer surfaces using bipolar electrochemistry, *Polym. J.*, 2016, **48**, 39–44.
- 101 T. M. Braun and D. T. Schwartz, Localized Electrodeposition and Patterning Using Bipolar Electrochemistry, *J. Electrochem. Soc.*, 2015, **162**, D180–D185.
- 102 Z. Fattah, P. Garrigue, V. Lapeyre, A. Kuhn and L. Bouffier, Controlled Orientation of Asymmetric Copper Deposits on Carbon Microobjects by Bipolar Electrochemistry, *J. Phys. Chem. C*, 2012, **116**, 22021–22027.
- 103 Y. Ishiguro, S. Inagi and T. Fuchigami, Gradient Doping of Conducting Polymer Films by Means of Bipolar Electrochemistry, *Langmuir*, 2011, **27**, 7158–7162.
- 104 S. E. Fosdick, K. N. Knust, K. Scida and R. M. Crooks, Bipolar Electrochemistry, *Angew. Chem., Int. Ed.*, 2013, **52**, 10438–10456.
- 105 Z. Ma, L. Fuentes-Rodriguez, Z. Tan, E. Pellicer, L. Abad, J. Herrero-Martín, E. Menéndez, N. Casañ-Pastor and J. Sort, Wireless magneto-ionics: voltage control of magnetism by bipolar electrochemistry, *Nat. Commun.*, 2023, **14**, 6486.
- 106 A. Jain, J. Gosling, S. Liu, H. Wang, E. M. Stone, S. Chakraborty, P. S. Jayaraman, S. Smith, D. B. Amabilino, M. Fromhold, Y.-T. Long, L. Pérez-García, L. Turyanska, R. Rahman and F. J. Rawson, Wireless electrical–molecular quantum signalling for cancer cell apoptosis, *Nat. Nanotechnol.*, 2023, **19**, 106–114.
- 107 J. S. Park, K. Park, H. T. Moon, D. G. Woo, H. N. Yang and K. H. Park, Electrical Pulsed Stimulation of Surfaces Homogeneously Coated with Gold Nanoparticles to Induce Neurite Outgrowth of PC12 Cells, *Langmuir*, 2009, **25**, 451–457.
- 108 C. Qin, Z. Yue, Y. Chao, R. J. Forster, F. O. Maolmhuaidh, X. Huang, S. Beirne, G. G. Wallace and J. Chen, Bipolar electroactive conducting polymers for wireless cell stimulation, *Appl. Mater. Today*, 2020, **21**, 100804.
- 109 F. J. Rawson, C. L. Yeung, S. K. Jackson and P. M. Mendes, Tailoring 3D Single-Walled Carbon Nanotubes Anchored to Indium Tin Oxide for Natural Cellular Uptake and Intracellular Sensing, *Nano Lett.*, 2013, **13**(1), 1–8.
- 110 L. Perez-Caballero, H. Carceller, J. Nacher, V. Teruel-Marti, E. Pujades, N. Casañ-Pastor and E. Berrocoso, Induced Dipoles and Possible Modulation of Wireless Effects in Implanted Electrodes. Effects of Implanting Insulated Electrodes on an Animal Test to Screen Antidepressant Activity, *J. Clin. Med.*, 2021, **10**, 4003.
- 111 B. S. Spearman, A. J. Hodge, J. L. Porter, J. G. Hardy, Z. D. Davis, T. Xu, X. Zhang, C. E. Schmidt, M. C. Hamilton and E. A. Lipke, Conductive interpenetrating networks of polypyrrole and polycaprolactone encourage electrophysiological development of cardiac cells, *Acta Biomater.*, 2015, **28**, 109–120.
- 112 S. L. Swisher, M. C. Lin, A. Liao, E. J. Leefflang, Y. Khan, F. J. Pavinatto, K. Mann, A. Naujokas, D. Young, S. Roy, M. R. Harrison, A. C. Arias, V. Subramanian and M. M. Maharbiz, Impedance sensing device enables early detection of pressure ulcers in vivo, *Nat. Commun.*, 2015, **6**, 6575.
- 113 A. J. Robinson, A. Jain, R. Rahman, S. Abayzeed, R. J. M. Hague and F. J. Rawson, Impedimetric Characterization of Bipolar Nanoelectrodes with Cancer Cells, *ACS Omega*, 2021, **6**, 29495–29505.
- 114 P. J. Sonneveld, W. Visscher, F. Panneflek and E. Barendrecht, The conductance of suspensions with conducting particles, *J. Appl. Electrochem.*, 1992, **22**, 935.
- 115 K. Percin, B. Vander Zee and M. Wessling, On the Resistances of a Slurry Electrode Vanadium Redox Flow Battery, *ChemElectroChem*, 2020, **7**, 2165.
- 116 M. Culebras, C. M. Gómez and A. Cantarero, Review on Polymers for Thermoelectric Applications, *Materials*, 2014, **7**, 6701–6732.
- 117 G. Salinas, S. Arnaboldi, P. Garrigue and A. Kuhn, Controlled Patterning of Complex Resistance Gradients in Conducting Polymers with Bipolar Electrochemistry, *Adv. Mater. Interfaces*, 2023, **10**, 2202367.
- 118 K. Yang, S. J. Yu, J. S. Lee, H. R. Lee, G. E. Chang, J. Seo, T. Lee, E. Cheong, S. G. Im and S. W. Cho, Electroconductive nanoscale topography for enhanced neuronal differentiation and electrophysiological maturation of human neural stem cells, *Nanoscale*, 2017, **9**, 18737.

